APPENDIX B: MODELING THE POTENTIAL EFFECTS OF CHANGED WATER AVAILABILITY AND TEMPERATURE ON THE SUMMER CHINOOK SALMON CULTURE PROGRAM AT ENTIAT NATIONAL FISH HATCHERY

Kyle C. Hanson[1] and Douglas P. Peterson[2]

[1]US Fish and Wildlife Service, Columbia River Fish and Wildlife Conservation Office,
1211 SE Cardinal Court, Suite 100, Vancouver, WA 98683

[2]US Fish and Wildlife Service, Abernathy Fish Technology Center,
1440 Abernathy Creek Road, Longview, WA 98632

Original draft: 12/20/19
Previous revision date: 07/09/2020
Current revision date: 06/25/2021

[1] Email: Kyle_Hanson@fws.gov
[2] Email: Doug_Peterson@fws.gov

ABSTRACT

Future climate conditions may inhibit the ability of salmon hatcheries in the Pacific Northwest to operate under long-established rearing schedules and fish production targets. Here, we evaluate the vulnerability of the Summer Chinook Salmon (*Oncorhynchus tshawytscha*) program at Entiat National Fish Hatchery (NFH) to future climates expected by the 2040s under a suite of 10 general circulation models (GCMs) and a 'middle-of-the-road' (A1B) greenhouse gas emissions scenario (IPCC 2007). We summarized projected environmental conditions in the Entiat River basin in Washington State and developed a temperature-driven growth model for hatchery-reared salmon that allowed us to evaluate monthly changes in mean fish size, water flow index (FI), and fish density index (DI) in the hatchery. We evaluated hatchery operations under future environmental conditions based on modeling the hydrology and temperature of the Entiat River, a regression relationship between surface and ground water temperatures, and a set of scenarios based on varying assumptions of connectivity between surface and groundwater hydrology. By the 2040s, mean annual water temperature in the Entiat River (8.7 °C) is expected to be about 1.2 °C warmer on average than the empirical historic mean (2001 – 2006) and the modeled historic mean (1915 – 2006). Major hydrologic changes are projected for the Entiat River with earlier snowmelt runoff, lower flows and more extreme droughts in summer, higher average flows in winter, and more extreme floods. Entiat NFH uses groundwater from wells to rear juvenile Summer Chinook Salmon for much of their production cycle (most importantly in summer). The use of ground water in summer resulted in much more modest increases in rearing water temperatures (+0.1 – 0.2 °C) than would be expected if the hatchery relied exclusively on surface water from the Entiat River. Overall, juvenile Chinook Salmon were projected to be approximately 15.6% heavier and 4.9% longer on average at release due to faster growth rates. The FI value in summer tended to be above the threshold value of 0.6 under the historical and most of the future scenarios we considered. Overall, the hatchery's use of groundwater in months when hydrologic modeling predicts that future surface water flows may be dramatically lower and warmer appeared to buffer threats to juvenile Chinook Salmon based on elevated flow index. However, this effect could be diminished if reductions in surface flows strongly affected groundwater availability. The DI exhibited little change relative to historic conditions for the future scenarios we modeled and remained below the 0.2 threshold value. Maintaining an adequate supply of cold ground water appears central to the hatchery's ability to rear salmon in the coming decades. A better understanding of the hydrologic connectivity between the Entiat River and hatchery wells would facilitate mitigation planning. Given the projected increases in mean winter flows and the magnitude of large floods in the Entiat River, a formal assessment of the threat to hatchery infrastructure posed by extreme high flow events may prove useful as well. Developing strategies or infrastructure to use groundwater more efficiently may further increase resilience to hydrologic and thermal changes projected for the Entiat River during summer.

INTRODUCTION

Pacific salmon (*Oncorhynchus* spp.) have a complicated life cycle and may be sensitive to the effects of climate change through a number of pathways. Changes in air temperature and precipitation patterns may cause the freshwater rearing habitat to become unsuitable due to altered thermal and hydrologic regimes (Mantua et al. 2010). Increased frequency and duration of fire in the western U.S. (e.g., Westerling et al. 2006) may alter disturbance regimes and influence the structure and function of some aquatic systems (e.g., Bisson et al. 2003; Isaak et al. 2010). Temperature increases in mainstem rivers can create seasonal thermal migration barriers that block adults from reaching spawning habitats (Mantua et al. 2010). The establishment of new invasive species and spread of existing ones that impact Pacific salmon will depend, to some extent, on how freshwater habitats are affected by climate change (Petersen and Kitchell 2001; Rahel and Olden 2008; Carey et al. 2011). Changes in ocean temperature, upwelling (e.g., Scheuerell and Williams 2005), and acidification (e.g., Fabry et al. 2008) could dramatically alter marine food webs that salmon depend on during the ocean phases of their life cycle.

The viability of wild (naturally spawning) and propagated (hatchery reared) populations of Pacific salmon could be affected by some or all of the aforementioned factors. A comprehensive analysis of all of those effects is highly desirable, but beyond the scope of the effort presented here. Rather, our intent is to focus in significant detail on one portion of the life cycle of hatchery-propagated salmon – that portion which takes place in the hatchery – to understand how growth rates, mean size, and total biomass of the cultured fish during that freshwater phase are affected by changes in water availability and temperature anticipated under future climates. This emphasis is based on two premises. First, the freshwater rearing phase of the salmon life cycle could represent a population bottleneck if climatic changes result in conditions that meet or exceed a species' physiological tolerances. This premise should be valid whether the rearing phase occurs in a hatchery or in a natural setting. Second, hatchery managers have some ability to influence rearing conditions within a hatchery in response to environmental perturbations. The hatchery represents an environment, albeit artificial, over which the U.S. Fish and Wildlife Service (USFWS) Fish and Aquatic Conservation program can design and implement climate mitigation and adaptation strategies.

Given these premises, our overall goal is to understand whether hatchery programs can operate in a 'business as usual' paradigm following existing fish-culture schedules and production targets under future climatic conditions, focusing specifically on changes in water temperature and water availability at the hatchery. Specific objectives are to: (a) determine if future environmental conditions are likely to altogether preclude propagation of certain species or populations, (b) identify the magnitude and timing of sub-lethal effects that may affect freshwater growth and survival, including the incidence of disease, and (c) suggest general mitigation and adaptation strategies given the impacts detected in (a) and (b). To achieve these objectives, we collated physiological tolerance data from the scientific literature for Pacific salmon species, adapted a temperature-driven growth model to predict fish growth, and

developed a modeling framework using flow index and density index parameters (Piper et al. 1982; Wedemeyer 2001) which integrate the effects of changing water temperatures and availability with fish growth, physiological stress, and disease risks.

Here, we applied our methodology to the Summer Chinook Salmon (*O. tshawytscha*) program at Entiat NFH, located on the Entiat River, a tributary to the Columbia River in north-central Washington State (Figure B1). We briefly summarized the important hydrologic changes anticipated for the Entiat River basin upstream from the hatchery. We then used empirical data on recent fish rearing conditions within the hatchery to predict the future growth, mean size and total biomass of salmon by (a) implementing the growth model and (b) modeling flow and density indices based on hatchery environmental conditions projected for the 2040s under a moderate, future greenhouse gas emission scenario (A1B scenario; IPCC 2007).

METHODS

Salmon thermal tolerances

In August 2011, a review of the peer reviewed literature of thermal tolerances of five focal species of Pacific salmon and anadromous trout (Chinook, Coho [*O. kisutch*], Chum [*O. keta*], and Sockeye [*O. nerka*] Salmon, and Steelhead [*O. mykiss*]) reared at National Fish Hatcheries (NFH's) in the Pacific Northwest was performed to determine the thermal tolerances for multiple life-history stages (Hanson and Peterson 2014)[3]. This information was acquired through two general approaches. First, to identify relevant primary literature, ISI's Web of Science (1985 – present) was searched for variations on the following key terms: *thermal tolerance*, *critical thermal maximum* (CTM), *incipient lethal temperature* (ILT), *temperature maximum* (TM), and *ultimate lethal incipient temperature* (UILT). Second, bibliographies from several reviews of thermal tolerance in fishes (Beitinger et al. 2000; Becker and Genoway 1979; Paladino et al. 1980; Beitinger and McCauley 1990; Lutterschmidt and Hutchinson 1997) were surveyed to locate additional information on each focal species. Results were then screened for relevance before inclusion in the literature review, and studies that did not specifically contain information on the thermal tolerance of the focal species were excluded from further synthesis. We attempted to extract the following thermal tolerance data (Elliott 1981) from results, tables and figures:

1. *Optimal temperatures*: the temperature range that allows for normal physiological response and behavior without thermal stress symptoms;
2. *Optimal growth temperatures*: the temperature range that provides the highest growth rates given a full food ration;

[3] See Online Resource 1 of Hanson and Peterson (2014) for list of references, available at: https://link.springer.com/article/10.1007/s00267-014-0302-2 .

3. *Optimal spawning temperatures*: the temperature range that results in lowest pre-spawn mortality and the highest fertilization rates and egg/embryo survival;
4. *Upper smoltification temperature limit*: the minimum, upper temperature at which the smoltification process is inhibited;
5. *CTM, ILT, or UILT*: the maximum temperature that induces 50% mortality in the fish previously acclimated to a given constant temperature.

Meta-data available varied among publications, but, to the extent possible, the following variables were recorded for each datum: life-history stage, fish length (mean ± SD or range in mm), fish weight (mean ± SD or range in g). When provided, the following supplemental meta-data from published values of CTM, ILT, or UILT tests was also recorded to facilitate proper interpretation of results: acclimation temperature (°C), maximum temperature from CTM, ILT, or UILT tests (°C), and test endpoint criterion. Thermal tolerance data for each species were categorized by the following three life-history stages[4]: (1) egg/fry, (2) juvenile, and (3) adult broodstock. Data were averaged for each of the three life-history stages to determine representative thermal tolerances for each life-history stage of Summer Chinook Salmon at Entiat NFH (Table B1).

Disease thermal tolerances

In August 2011, we reviewed the peer-reviewed scientific literature on thermal tolerances of common pathogens that infect salmon at aquaculture facilities in the Pacific Northwest to determine the range of temperatures at which each pathogen is known to cause disease (Hanson and Peterson 2014). The literature review followed the same protocols as described above, but with the common name or Latin binomial of each pathogen added to the following search terms: *thermal tolerance*, *outbreak temperature*, and *transmission temperature*. Results were then screened for relevance before inclusion in the literature review, and studies that did not specifically contain information on the thermal tolerance of the focal species were excluded from further synthesis. Several references provided detailed information for the following two variables (Table B2):[5]

1. *Disease outbreak temperatures*: The pathogen-specific temperature range at which disease and mortality are most likely in Pacific salmon and Steelhead; and
2. *Minimum disease temperatures*: The lowest temperature (or range) at which the pathogen-specific disease occurs in Pacific salmon and Steelhead.

---

[4]These three life-history stages are the principle ones addressed by salmon hatcheries in the Pacific Northwest. Egg/fry include fertilized eggs, sac fry, and fish less than 70 mm total length. Juvenile fish are sexually immature fish in large rearing containers (e.g., raceways) prior to release. Adult broodstock are sexually mature fish that have returned to the facility during the spawning migration.

[5] See Online Resource 1 of Hanson and Peterson (2014) for list of references, available at: https://link.springer.com/article/10.1007/s00267-014-0302-2 .

Water sources for Entiat NFH

Entiat NFH uses a combination of surface and groundwater to rear salmon (see Table 1 in main report). The hatchery has a surface and groundwater right (certificate #3058, priority date June 4, 1943, and amended February 21, 1996) to 22.5 cfs from the Entiat River and six on-site wells. The facility also has access to Packwood Spring (aka Limekiln Spring, certificate #3059, priority date June 4, 1943) for 7.0 cfs. Surface water is diverted from the Entiat River to the hatchery via an intake pipe approximately 0.6 miles (1 km) upstream of the hatchery property (Figure B2). The six supply wells used by Entiat NFH vary from 75 to 130 feet deep. Groundwater is utilized at specific times in the rearing cycle, and the wells provide variable average amounts of water for fish production (#1 = 350 gpm, #2 = 200 gpm, #3 = 375 gpm, #4 = 275 gpm, #5 = 125 gpm, and #6 = 100 gpm). Groundwater from the well sources is mixed in an aeration building prior to distribution to rearing units.

We obtained historical surface water temperatures by conducting data calls with staff from Entiat NFH and the USFWS Water Resource Branch. The staff at Entiat NFH provided a dataset of water temperatures during 2001 – 2006 based on readings taken every 15 – 60 min by a temperature logger deployed in the Entiat River adjacent to the hatchery. The USFWS monitors water temperature at the hatchery, and a reasonably complete record of temperature data since 2000 is available (Table B3, left column).[6] To represent water conditions experienced by fish in the hatchery and to project future conditions, we needed to account for all the constituent water sources and their potential mixing. We were thus interested in temperatures and discharge (or water use) from the groundwater wells and Entiat River.

Surface water temperatures upstream from Entiat NFH

When salmon are being reared with surface water only, water temperatures at the hatchery intake are assumed representative of the thermal conditions within the hatchery rearing units. We established a regression relationship between air temperature and water temperature using the method of Mohseni et al. (1998) following the approach of Mantua et al. (2010). This relationship was used to simulate both historical and future water temperatures at the hatchery intake. The non-linear regression model of Mohseni et al. (1998) is intended for use with weekly time-series data and takes the form,

$$T_{sw} = \mu + \frac{\alpha + \mu}{1 + e^{\gamma(\beta - T_{air})}}$$

where T_{sw} = surface water temperature, μ = estimated minimum stream temperature, α = estimated maximum stream temperature, γ = a measure of the steepest slope of the function, β = the air temperature at the inflection point of the function, and T_{air} = measured air temperature. Mean weekly air temperature for the Entiat River watershed was estimated from historic air

[6] Data are missing for some years and months due to loss or malfunction of thermographs.

temperatures downscaled from general circulation models (aka global climate models or GCMs)[7] by aggregating the daily mean air temperatures within the area of overlap between the 1/16° grid cells (scale of the downscaled historic climate data) and the Entiat River watershed boundary upstream from Entiat NFH, as delineated by a Geographic Information System (GIS; see Figure B3). Consequently, we refer to the historic air temperatures as area-weighted values.

The modeled historical air temperature data covers the period of 1915 – 2006, and we fit the regression model using data from a period of temporal overlap between the modeled air and empirical water temperatures from 2001 – 2006. We fit the models with the non-linear regression package 'nls' in R version 3.2.3 (R Core Team 2015), and assumed a stable mathematical relationship (i.e., with fixed-value parameters) between weekly average air and surface water temperatures.

The resulting model fit had a Nash-Sutcliffe coefficient of 0.882 (NSC, Nash and Sutcliffe 1970), and we did not find any evidence that we needed to account for hysteresis (NSC = -2.8 for hysteresis model). The model's parameter estimates yielded the following equation to predict water temperatures (T_{sw}) at the Entiat River adjacent to the hatchery as a function of mean air temperature (°C) over the watershed upstream of the hatchery:

$$T_{sw} = 0 + \frac{19.19 + 0}{1 + e^{0.19(7.66 - T_{air})}}$$

Predicted weekly historic surface water temperatures in the Entiat River adjacent to the hatchery were generated from the preceding equation by entering the downscaled historic air temperatures (1915 – 2006), whereas the weekly surface water predictions for the 2040s were generated by entering the statistically downscaled[8] air temperature predictions from an ensemble of ten GCMs – ccsm3, cgcm3.1_t47, cnrm_cm3, echam5, echo g, hadcm, hadgem1, ipsl_cm4, miroc_3.2, and pcm1 – forced by the A1B emissions scenario (Hamlet et al. 2010a, b). The A1B scenario is often referred as "middle-of-the-road" in terms of emissions levels and projected warming, and has been utilized as a reference in a number of studies (e.g., Mantua et al. 2010; Wenger et al. 2011). The A1B scenario assumes that some global efforts are undertaken in the 21st Century to reduce the rate of increase in greenhouse gas emissions compared to the 1980 – 1999 baseline established in the 4th IPCC Assessment Report (IPCC 2007).[9]

---

[7] Flux files from: http://warm.atmos.washington.edu/2860 .

[8] Data were downscaled using the hybrid delta method (see Hamlet et al. 2010b).

[9] The A1B scenario and other global model outputs of the 4th IPCC (IPCC 2007) have recently been supplanted by a new set of scenarios and modeled outputs from the 5th IPCC (IPCC 2014). The A1B is referred to as a SRES scenario described in the Intergovernmental Panel on Climate Change (IPCC) Special Report on Emissions Scenarios (IPCC 2000). A1B is one of a family of scenarios used in fourth global climate assessment (AR4) that describe greenhouse gas emissions under alternative developmental pathways assuming different future expectations for demographic, economic, and technological outcomes with no additional climate policies (IPCC 2007). The most recent IPCC global climate assessment (AR5) uses a different methodology to describe global climate forcing, called Representative Concentration Pathways or RCPs (IPCC 2014). The RCPs represent trajectories for greenhouse gas emissions and other atmospheric elements that affect the radiative forcing of the earth's climate

Groundwater temperatures at Entiat NFH

We performed exploratory linear regression analyses to determine if monthly well temperatures were correlated with surface water temperatures recorded at the Entiat NFH intake. Our objective was to determine if we needed to account for monthly variation in well temperatures and provide a basis for translating projected changes in the Entiat River temperatures to potential changes in well temperatures. We found that the well temperatures were correlated with mean monthly surface water temperatures when factoring in a three-month lag ($P < 0.001$, d.f. = 1, 10, $R^2 = 0.82$) in the following equation:

$$T_{GW} = 8.693 + (0.110 \times T_{SW})$$

wherein T_{GW} is the monthly mean water temperature measured in the groundwater wells and T_{SW} is the monthly mean surface water temperature in the Entiat River adjacent to the hatchery three months earlier.

Growth Model Simulation

We used the fish growth model of Iwama and Tautz (1981) to estimate how the growth of Summer Chinook Salmon reared in Entiat NFH might change in response to future climate. This model has been widely applied to evaluate growth of captive salmonids (Dumas et al. 2007; Good et al. 2009; Jobling 2010), and we used it here to estimate mean fish size at age (month of year) as a function of water temperature assuming an unlimited food ration. We solved the equation to estimate mean fish weight at time-step i (W_i) as:

$$W_i = \left[W_0^b + \left(\frac{T_i}{10^3} \right) \bullet d_i \right]^{\frac{1}{b}}$$

where W_0 is initial weight (g), and T_i and d_i are the average temperature and number of days in time-step "i". Iwama and Tautz (1981) analyzed growth data for three species of salmonid fishes and proposed that $b = 0.33$ provided a reasonable approximation that balanced model accuracy and simplicity. Consequently, we applied that exponent in our analyses. To estimate mean fish length (L_i) by time-step, we rearranged an equation for Fulton-type fish condition factor (Anderson and Gutreuter 1983) to solve for fish fork length (L_i in mm) as:

---

through time and assume possible mitigation actions (van Vuuren et al. 2011). The AR5 assessment uses four representative RCPs: RCP2.6, RCP4.5, RCP6, and RCP8.5 in rank order of their radiative forcing and emission levels (van Vuuren et al. 2011; IPCC 2014). The SRES A1B scenario falls roughly between the RCP6 and RCP8.5 (though closer to RCP6) in terms of CO_2 concentration, radiative forcing, and expected increases in mean global temperatures (van Vuuren and Carter 2014). We acknowledge the updated and improved assessments of AR5 (IPCC 2014) but have relied here on the outputs of the A1B scenario of AR4 (IPCC 2007) for our vulnerability assessment of Entiat NFH to maintain quantitative consistency with our previous and other ongoing vulnerability assessments of NFHs in the Pacific Northwest.

$$L_i = \left(\frac{W_i}{K / 10^5} \right)^{1/3}$$

where K is the condition factor which was held constant at $K = 1.0$ to represent healthy fish.

We applied the growth model to estimate monthly mean fish sizes of Summer Chinook Salmon starting with the first July after hatch when fish are marked. The initial weight at marking was the input for the first month in the growth simulation, and subsequent months were initialized using the predicted final weight of the fish from the preceding month. The growth model was implemented with hatchery thermal environments consistent with recent historical conditions and the scenario projected for the 2040s. We then compared cumulative differences in mean size of Chinook Salmon between historical and projected thermal regimes.

Flow index and density index: critical fish-culture parameters

Hatcheries typically operate to achieve production targets (mean weight and total number of fish at release) while remaining below threshold flow and density index values established as fish health guidelines based on empirical observations of fish disease, mortality, or poor growth. These indices function as general rules of thumb based on oxygen saturation for different water temperatures and elevation (e.g., Piper et al. 1982) and act as surrogates for carrying capacity within the facility. Conceptually, these indices are the total fish biomass divided by the product of mean fish length and either (a) water use (flow index [FI]) or (b) total rearing volume or capacity (density index [DI]):

$$FI_i = \frac{N_i \bullet W_i}{L_i \bullet GPM_i}$$

and

$$DI_i = \frac{N_i \bullet W_i}{L_i \bullet C_i}$$

where FI_i and DI_i are flow and density indices, respectively, N_i is the total number of fish (abundance), W_i is mean fish weight (lbs), L_i is mean fish length (in), GPM_i is water use rate by the hatchery (gallons per minute), and C_i is the rearing capacity (ft^3) at monthly time-step i. In this formulation, mean fish length (L_i) and weight (W_i) are forced by water temperature (T_i) in the growth model above, thereby linking temperature and climate changes to variation in FI_i and DI_i. Flow index also changes in response to water availability (GPM_i). Rearing capacity (C_i) does not necessarily change in response to climate, but could be adjusted by managers to compensate for the effect of increased fish growth on DI_i.

Integrating the effect of water temperature and water availability on hatchery operations

We used flow index and density index as response variables to integrate and evaluate the combined effects of changing water temperatures, water availability, and physical rearing capacity at Entiat NFH (and more generally, as surrogates for carrying capacity under historical and future conditions). To do this, we used both recent historical conditions and climate model output for the 2040s to drive the salmon growth model and to simulate flow and density indices for Chinook Salmon at Entiat NFH in each monthly time-step after initial ponding. This produced monthly values for each index at each time-step (modeled historical and modeled future values). The modeled historical and empirical FI_i and DI_i values recorded in the hatchery could differ because of real-time changes implemented by hatchery managers, such as reducing feed rations or increasing hatchery water use in response to environmental conditions. We could not explicitly represent those variable factors in the analyses, so we adjusted the future simulated values based on the ratio between the empirical and modeled historical values (rFI_i and rDI_i) as:

$$rFI_i = \frac{FI_i \ mean\ empirical\ historical}{FI_i \ modeled\ historical}$$

$$rDI_i = \frac{DI_i \ mean\ empirical\ historical}{DI_i \ modeled\ historical}$$

Thus, the future bias-corrected index values were:

$$FI_i \ future\ corrected = rFI_i \bullet FI_i \ modeled\ future$$

$$DI_i \ future\ corrected = rDI_i \bullet DI_i \ modeled\ future$$

A complete description of the model formulation and underlying equations are presented in Hanson and Peterson (2014).[10]

To generate estimates for water availability at Entiat NFH under the A1B emissions scenario that could be used could be used to estimate flow indices, we used a combination of simulated streamflow data from the variable infiltration capacity (VIC) hydrologic model (Liang et al. 1994) and scenarios that made different assumptions about how climate change affected the wells and how the hatchery utilized water. For surface flows, we used VIC data forced by output from the same 10 GCM ensemble used to derive water temperatures (e.g., Mantua et al. 2010). Streamflow data were summarized as mean monthly surface water discharge in the Entiat River routed to the location of Entiat NFH (A. Hamlet, Climate Impacts Group, University of

[10] Note: $rDI_i = rFI_i$ (= r_i) at each time step because (a) the value of N_iW_i/L_i is the same for calculating DI_i and FI_i at each time step for each scenario (i.e., N_iW_i/L_i differs between modeled historical and empirical scenarios but not between DI_i and FL_i for each scenario), and (b) the values for GPM_i and C_i, respectively, at each time step were the same in both scenarios (i.e., the modeled historical scenario used the same values of GPM_i and C_i, respectively, as those measured empirically).

Washington, unpublished data). While Entiat NFH reports that the groundwater wells yield slightly less water when flows in the Entiat River drop to between 100 – 150 cfs (C. Chisam, Entiat NFH, pers. comm., March 23, 2020), we did not have enough information to develop a quantitative, predictive relationship between surface flows and well output. Given the uncertainty about how future surface water flows will affect groundwater, we modeled flow index using a set of scenarios for the 2040s that made different assumptions about how groundwater will be affected and the ability of the hatchery to utilize water. Scenario A assumed a *status quo* where there were no changes in water available to the hatchery, such that water use in 2040s is the same as the recent average for brood years 2013 – 2017. Scenario B assumed that surface water available to the hatchery would change (increase or decrease) in proportion to mean flows in the Entiat River[11], but the availability of well water would not change. Scenario C assumed the hatchery could utilize more surface water in months when Entiat River flows were projected to increase, but that reliance on wells would buffer any potential reduction in water availability in months when surface flows were projected to decrease. Scenario D makes the more pessimistic assumptions that any reductions in surface water flows will result in proportional decreases in water availability from wells, and that the hatchery cannot utilize additional water in months when surface flows are projected to increase.

RESULTS

Projected future climate in the Entiat River basin and at Entiat NFH under the A1B emissions scenario

Under the A1B emissions scenario by the 2040s, the Entiat River basin is projected to experience, (a) warmer air and water temperatures, (b) reduced snowpack and earlier snowmelt runoff, (c) lower base flows and more extreme low flow events in summer, and (d) higher flows in winter and larger magnitude floods (Tables B3 – B5; Figures B4 – B15). Mean air temperature over the entire watershed was expected to increase in every month (mean ± S.D. = 2.0 ± 0.5 °C) with the largest absolute increases predicted for July – September (range 2.6 – 3.0 °C; Table B4 and Figure B4). Total annual precipitation was projected to be within about 6% of the historical baseline (historical: 83 mm, 2040s: 88 mm). Monthly historical precipitation generally fell within the range of predictions from the 10 GCMs, except for July where the 2040s was expected to be slightly drier and November when the 2040s was expected to be wetter (Table B4; Figure B5). Maximum snow water equivalent (SWE, aka snow pack) in April was predicted to decline by nearly 26%, from 433 mm to 322 mm. For every month except December, the 2040s SWE estimates for all 10 GCMs were lower than the historical values, and the mean monthly SWE was predicted to decline by 29% in the 2040s compared to the historic

[11] For example, if the hatchery utilized 100% surface water in a given month and historically used 10 cfs but surface flows in that month were projected to decline by 40%, then the water available to salmon rearing in the future would be 10 cfs × 0.6 = 6 cfs)

baseline values (mean historical monthly mean = 177 mm, 2040s monthly mean = 125 mm; Table B4; Figure B6).

Based on the VIC modeling, mean annual flows projected for the Entiat River in the 2040s were higher than modeled historical values (historical = 653 cfs, 2040s ensemble mean = 729 cfs), and projections for 8 of 10 GCMs were greater than the historical mean (Table B5). The same pattern is apparent when the flow data are plotted by stream segment across the contributing basin (Figure B7). In addition to a projection for higher mean annual flow, the shape of the modeled hydrograph for the 2040s differs considerably from the simulated historic average (Figure B8). The projected Entiat River hydrograph at the location of the hatchery shows lower flows June through August (Figures B8 – B9) with an average flow decrease of 38.5% (range -20.0% to -56.5%) compared to the historic average. In contrast, mean flows of the Entiat River in the 2040s at the hatchery in late fall through spring (November – April) were projected to increase by an average of 65.0% (ensemble range 53.7 – 113.8%; Figures B8 – B9). The month of peak flow was projected to shift from June to May (Figure B8). The modeled historic hydrograph is similar in shape to the observed hydrograph for 1996 – 2019 based on USGS gage #12452990, except the observed hydrograph's month of peak flow is May instead of June (Figure B8).

The date at which half the annual discharge passes a particular point was projected to be more than at least 18 days earlier in the 2040s for the mainstem Entiat River and most of the river basin upstream from the hatchery (Figure B10). In general, summer low flow events (7Q10) were projected to be more severe in the mainstem and upper portions of the Entiat River basin (Figure B11), and the 7Q10 flow at Entiat NFH was projected be 2.6 cfs lower on average (Figure B12). In winter, the number of *W95* days – defined as the number of days in a calendar year when surface flows are in the top 5% of annual daily flows – were projected to increase by more than 2.5 days at the site of the hatchery (Figure B13). The magnitude of high flows with recurrence intervals of 20, 50, and 100 years was expected to increase with high certainty by the 2040s, with the largest floods (100 year recurrence interval) projected to increase from about 8,020 cfs to 13,658 cfs (a 70% increase), on average (Figure B14).

Water temperature in the Entiat River adjacent to Entiat NFH is projected to be warmer in most months in the 2040s compared to the historical period (Table B6; Figure B15). The mean annual water temperature was projected to increase by an average of 1.2 °C (range of monthly increase = 0.7 – 1.9 °C), and mean monthly temperature in July and August was projected to meet or exceed 16.5 °C. The largest mean annual water temperature increases are projected for May (1.6 °C), August (1.5 °C), September (1.9 °C) and October (1.5 °C) (Table B6; Figure B15). Mean groundwater temperatures in the 2040's are projected to increase between 0.07 and 0.2 °C in all months when compared to the historical baseline (Table B7).

Summer Chinook Salmon program

Capture of adult Chinook Salmon for broodstock at Entiat NFH typically starts in July and continues until spawning in October (Table B7). The adult holding ponds are supplied with 100% groundwater at this time. By the 2040s, the water temperatures in holding ponds are predicted to increase by between 0.15 °C and 0.2 °C (Table B7; Figure B16). The projected maximum increase in temperatures to 10.5 °C by the 2040s does not exceed the optimal spawning temperatures for Chinook Salmon (5.7 – 11.7 °C) based on literature values (Table B1), from which we infer it is unlikely adult Chinook will experience physiological stress during holding and spawning due solely to temperature.

Juvenile Chinook Salmon reared in Entiat NFH will be exposed to warmer rearing conditions by the 2040s, with projected increases ranging between 0.03 °C and 1.6 °C across the rearing periods (October year 1 to April year 2; Table B7, Figure B17). Increases of more than 1.0 °C are projected for November (+1.2 °C), December (+1.6 °C), and January (+1.2 °C) of the second rearing year when fish are exposed to a blend of groundwater and surface water. By the 2040s, water temperatures are projected to remain within the optimal temperatures for eggs/fry and below the upper optimal temperature threshold for juveniles during rearing at Entiat NFH (cf. Table B1 and Figure B17). At the time of release, the future water temperature within the facility in April (7.8 °C) is also projected to remain well below the upper limit for proper smoltification (14.0 °C; Table B7). These temperatures are also below the optimal growth temperatures for common salmon pathogens except for bacterial coldwater disease (Table B2 and Table B7), although higher water temperatures generally increase disease risks.

While the predicted 2040s temperatures in the hatchery will not exceed physiological tolerances of Chinook Salmon, warmer water temperatures will increase growth rates of juvenile Chinook Salmon throughout the rearing period compared to the historic baseline (Table B8). The largest increases in mean weight and length of Chinook Salmon juveniles are predicted to occur in the months when fish are reared on a blend of groundwater and surface water in the second rearing year (December – April). Chinook Salmon smolts from Entiat NFH are predicted to be, on average, 15.6% heavier and 4.9% longer at release compared to historical sizes (Table B8).

The historic flow index value for Summer Chinook Salmon often exceeded the threshold guideline value of 0.6 during July – October when fish are reared exclusively on well water (Table B9A; Figure B18). All of the future water availability scenarios modeled showed a similar pattern during that time, with Scenario D being the most pessimistic by assuming that well water availability was proportionally reduced by decreases in surface flows in the Entiat River. Flow index increased slightly under Scenario A (*status quo* for water availability) due to greater fish growth from higher water temperatures. During November – April when fish are reared on mostly surface water, the flow index generally below the 0.6 threshold value for all scenarios (Table B9B). During this time, flow index actually decreased under Scenario B that assumed that more water could be utilized. Scenarios B and C produced identical results as a reduction in surface flows (which distinguish these two scenarios) had no effect due to the

hatchery's reliance on ground water in months where surface flows were projected to decrease. Assuming recent average rearing densities and rearing unit capacity continue into the future, the density index exhibited little change (relative to the recent average) by the 2040s and never exceeded the threshold value of 0.2 under historical or future conditions (Figure B18).

DISCUSSION

Climate projections indicate warmer air temperatures in the Entiat River basin and that mean surface water temperatures in the Entiat River should increase in every month by the 2040s. Hydrologic modeling forced by future climate conditions suggests that mean annual flow in Entiat River during the 2040s will be similar to the historic baseline, but that the shape of the annual hydrograph may be dramatically different with earlier peak flows, higher flows in winter and greater magnitude peak flows (i.e., 100-year floods). Conversely, lower baseflows with more frequent and intense droughts are projected during summer. Despite these projections, the anticipated effect of those changes on the ability of Entiat NFH to rear Summer Chinook Salmon appears minor under the conditions we modeled, with a few exceptions discussed below.

Rearing Summer Chinook Salmon at Entiat NFH under future conditions

The hatchery's utilization of groundwater during summer appears to buffer juvenile salmon rearing conditions to both potential increases in surface water temperatures and decreases in surface flows in the Entiat River. Based on recent observations, well water was 3.7 – 7.6 °C colder that surface water in the Entiat River during July – September (Table B6). Consequently, while mean surface water temperatures during July – September were projected to increase by 1.4 – 1.9 °C, the rearing water for juvenile Chinook Salmon was only projected to increase by a fraction of a degree (0.1 – 0.2 °C) because colder groundwater was not predicted to experience much warming.

Chinook Salmon smolts reared by Entiat NFH were predicted to be 4.9% longer and 15.6% heavier at release in the 2040s, and most of this difference appeared to result from growth during the final five months of rearing (November – April) when the hatchery uses primarily surface water (Table B8), albeit during a time when surface water is comparatively cold (< 8 °C, Table B7). These temperature-driven size increases would be much more pronounced if the hatchery also used warmer surface water from the Entiat River during summer. At a fundamental level, the hatchery's use of the colder groundwater appears to prevent rearing temperatures from exceeding the physiological thresholds for Chinook Salmon or inducing direct mortality via thermal stress (Table B1). Nevertheless, since juvenile Chinook Salmon experience disease outbreaks under the existing thermal regimes, the modest warming we projected for rearing water temperature at Entiat NFH may be of concern as warmer temperatures can impact immune function and increase susceptibility to pathogens.

Mean monthly summer flows in the Entiat River during June – August were projected to decline by 38.5% on average, but this had little effect on the modeled flow index values because the

hatchery was utilizing well water. However, under the historical operations and for the future scenarios we considered, the flow index value exceeded the threshold value of 0.6 in at least three of the four consecutive months July – October when fish were reared on 100% well water. The hatchery reports that the output from their wells can change slightly when water levels in the Entiat River are comparatively low (e.g., well output ~5% lower, C. Chisam, Entiat NFH, pers. comm., February 25, 2020). We modeled a more extreme scenario (D) that assumed an even stronger relationship between wells and surface flows such that well output decreased in direct proportion to river flows, and the flow index values predictably spiked (see Figure B18), implying lower water quality associated with lower water availability and potential increase risk of physiological stress and disease. Collectively, the projected future conditions in both the Entiat River and hatchery-rearing environment underscore the critical importance of ground water to rearing Summer Chinook Salmon, both now and in the 2040s.

If well output should decline substantially in summer, additional reliance on surface water from the Entiat River may not be a tenable option given the projected changes in flow, even if the water could be chilled or re-used. Currently, Entiat NFH must implement a negotiated flow conservation plan to help maintain instream flows based upon permitted thresholds throughout the year (C. Chisam, Entiat NFH, pers. comm., February 25, 2020). From May 1 through October 31, the hatchery's diversion of surface water cannot exceed 5% of mean daily flow at the USGS Entiat River gage whenever the combination of flow minus the amount of hatchery surface diversion is less than 200 cfs (C. Chisam, Entiat NFH, pers. comm., February 25, 2020). Hydrologic modeling for the 2040s project an ensemble mean monthly flow of 121 cfs in August and 105 cfs in September. Those projected flows would likely trigger more frequent implementation of the instream flow plan or its implementation for a longer duration, resulting in the hatchery not being able to utilize its full surface water right. Hatchery staff have observed reduced output (recharge rate) from the wells when surface flows are in the range of 100 – 150 cfs that could affect the number of fish reared during the summer by increasing flow indexes above guideline levels when groundwater is used exclusively. Loss of groundwater during August and September may affect salmon rearing by increasing the flow index. To compensate, serial re-use of diverted surface water could theoretically be employed to help maintain desired water flows in the hatchery, but the hatchery would not be able to divert its full water right and this water is already comparatively warm. Furthermore, re-use would further reduce water quality due to decreased oxygen levels and increased fish waste.

The hatchery also follows a negotiated flow conservation plan to help maintain instream flows during the winter months when precipitation falls as snow and the Entiat River has minimal flow (see Figure B8). From November 1 through April 30, the hatchery's diversion of surface water cannot exceed 10% of mean daily flow at the Entiat River gage whenever the combination of flow minus the amount of hatchery surface diversion is less than 100 cfs (C. Chisam, Entiat NFH, pers. comm., March 24, 2020). Hatchery staff report the flow conservation plan has been triggered numerous times in recent years. Interestingly, the future flows are predicted to be substantially higher during November – April (Figures B8 – B9). We attribute this to warming

air temperatures resulting in more precipitation falling as rain during the winter months as well as earlier snowmelt. This would result in the negotiated flow conservation plan covering November – April being implemented less frequently during the 2040s.

With respect to water availability, our modeling focused primarily on how changes to the natural environment might affect the amount of water that the hatchery is capable of using to rear juvenile Chinook Salmon. We did not model the effects of floods on hatchery infrastructure (and any resulting impact on fish culture) because such analyses were beyond the scope of our objectives. The hydrologic modeling does project dramatic increases in the magnitude of winter flows (e.g., Figures B8 – B9) and large floods (e.g., Figure B14), so a formal assessment of potential damage to infrastructure from peak flows of 8,000 – 14000 cfs in the Entiat River would be desirable for considering climate change adaptation strategies for Entiat NFH.

A few key assumptions and uncertainties

We did not formally consider how water re-use would affect water quality in rearing units, thus our calculations for flow index assume single-pass water of optimal quality based on its ambient temperature. The hatchery serially re-uses groundwater beginning in August when approximately two-thirds of the fish in the upper A bank are redistributed among the middle and lower B and C banks, respectively, with fish in B bank receiving reuse water from A bank, and fish in C bank receiving second-pass reuse water from B bank. Hence, our calculated flow index values may functionally overestimate water quality during those months when fish are receiving reuse water. In addition, for brood years 2016 and 2017, the hatchery serially re-used surface water to rear juveniles during November – April because of low flows of the Entiat River and icing of the water intake, thus preventing the hatchery from diverting its entire surface water right (C. Chisam, February 25, 2020, pers. comm.). Although our modeling suggests higher flows and warmer temperatures of the Entiat River in the 2040s from November through April, we are uncertain how those projected changes may affect the need of the hatchery to re-use surface water to keep flow index values from exceeding the threshold value.

The Entiat River and the hatchery wells appear to be hydraulically connected, but quantitative details regarding that connectivity are not available. We developed a regression relationship that allowed us to represent the future groundwater temperatures as function of future surface water temperature, so we could model directly the thermal environment experienced by salmon in the hatchery. In contrast, we did not have a means to quantify how changes in surface water flow in the Entiat River would affect output from the wells. We believe a functional relationship exists based on anecdotal observations of well recharge rates by hatchery staff, but we had no data to represent it. Rather, we modeled different scenarios that bounded optimistic or pessimistic alternatives, such as well output remaining unchanged despite projected hydrologic changes or well output declining proportionally to lower stream flow. Our results were clearly sensitive to these assumptions (e.g., see Figure B18), which highlights the need for more information about groundwater dynamics near the hatchery's wells given their importance to continued salmon production at the facility.

Mitigating the effects of climate change at Entiat NFH

The hatchery's current practice of using of cold groundwater to rear juvenile Chinook Salmon during summer is a significant pre-adaptation to projected future climate conditions in the Entiat River basin, and maintaining that supply of cold water will be even more important in coming decades. Understanding the relationship between surface flows in the Entiat River and the hatchery's wells – surface flow thresholds where well output decreases or stops, spatial and temporal patterns of groundwater recharge, etc. – may be critical information for hatchery management given the significant hydrologic changes projected for the Entiat River basin. Strategies for more efficient use of existing groundwater resources such as serial re-use or installation of recirculating aquaculture systems (RAS) might warrant evaluation.

Electro-mechanical chilling of surface water is possible, but it seems impractical to consider chilling enough water to rear ~450,000 Summer Chinook Salmon. Alternatively, a smaller volume of diverted surface water could be chilled to augment the well water supply during summer and keep flow index values below the 0.6 threshold. However, this presumes that instream flow conditions would permit the hatchery to utilize its surface water rights in the Entiat River.

Growth modulation through reduced rations is another mitigation option, although ration levels would need to ensure fish maintained adequate physiological condition and health. The growth rate of juvenile Chinook Salmon already appears to be somewhat low during October – February under current practices (see Table B9A), and we do not know if any additional scope remains to further limit fish growth without compromising their condition and ability to smolt. Finally, a direct and seemingly cost-effective means to lower flow and density indices would be to rear fewer fish, though this would need to be investigated in conjunction with sizing of other hatchery programs in the region to ensure that overall release goals decided through mandate and litigation are being met.

ACKNOWLEDGEMENTS

We thank Craig Chisam and the staff at the Entiat NFH for providing data and comments during the modeling process. Additional data was provided by Greg Fraser and Matt Cooper at Mid-Columbia Fish and Wildlife Conservation Office. The Region 1 NFH Climate Change Planning Team of Chris Pasley, Bill Gale, Patty Crandell and Don Campton provided general guidance on the scope and content of this project, and also contributed useful comments on this report. Ingrid Tohver (University of Washington, Climate Impacts Group) provided the modeled flow data generated by the distributed hydrologic (VIC) model and R code that we modified to predict water temperatures based on forcing data from global climate models.

REFERENCES

Anderson, R. O., and S. J. Gutreuter. 1983. Length, weight, and associated structural indices. Pages 283-300 in L. A. Nielson and D. L. Johnson, editors. Fisheries techniques. American Fisheries Society, Bethesda, Maryland.

Becker, C. D., and R. G. Genoway. 1979. Evaluation of the critical thermal maximum for determining thermal tolerance of freshwater fish. Environmental Biology of Fishes 4:245-256.

Beitinger, T. L., W. A. Bennett, and R. W. McCauley. 2000. Temperature tolerances of North American freshwater fishes exposed to dynamic changes in temperature. Environmental Biology of Fishes 58:237-275.

Beitinger, T. L., and R. W. McCauley. 1990. Whole-animal physiological processes for the assessment of stress in fishes. Journal of Great Lakes Research 16:542-575.

Bisson, P. A., B. E. Rieman, C. Luce, P. F. Hessburg, D. C. Lee, J. L. Kershner, G. H. Reeves, and R. E. Gresswell. 2003. Fire and aquatic ecosystems of the western USA: current knowledge and key questions. Forest Ecology and Management 178(1-2):213-229.

Carey, M. P., B. L. Sanderson, T. A. Friesen, K. A. Barnas, and J. D. Olden. 2011. Smallmouth bass in the Pacific Northwest: a threat to native species; a benefit for anglers. Reviews in Fisheries Science 19:305-315.

Dumas, A., J. France, and D. P. Bureau. 2007. Evidence of three growth stanzas in rainbow trout (*Oncorhynchus mykiss*) across life stages and adaptation of the thermal-unit growth coefficient. Aquaculture 267(1-4):139-146.

Elliott, J. M. 1981. Some aspects of thermal stress on freshwater teleosts. Pages 209-245 in: A. D. Pickering, editor. Stress and Fish. Academic Press, New York, NY.

Fabry, V. J., B. A. Seibel, R. A. Feely, and J. C. Orr. 2008. Impacts of ocean acidification on marine fauna and ecosystem processes. ICES Journal of Marine Science 65:414-432.

Good, C., J. Davidson, C. Welsh, B. Brazil, K. Snekvik, and S. Summerfelt. 2009. The impact of water exchange rate on the health and performance of rainbow trout *Oncorhynchus mykiss* in water recirculation aquaculture systems. Aquaculture 294(1–2):80-85.

Hamlet, A. F., E. P. Salathé, and P. Carrasco. 2010a. Statistical downscaling techniques for global climate model simulations of temperature and precipitation with application to water resources planning studies. Chapter 4 in Final Report for the Columbia Basin Climate Change Scenarios Project, Climate Impacts Group, Center for Science in the Earth System, Joint Institute for the Study of the Atmosphere and Ocean, University of Washington, Seattle.

Hamlet, A. F., P. Carrasco, J. Deems, M. M. Elsner, T. Kamstra, C. Lee, S.-Y. Lee, G. Mauger, E. P. Salathé, I. Tohver, and L. Whitely Binder. 2010b. Final Project Report for the Columbia Basin Climate Change Scenarios Project, http://www.hydro.washington.edu/2860/report/.

Hanson, K. C. and D. P. Peterson. 2014. Modeling the potential impacts of climate change on Pacific salmon culture programs: an example at Winthrop National Fish Hatchery. Environmental Management 54:433-448. Online Resource 2 available at: http://link.springer.com/article/10.1007/s00267-014-0302-2.

Hawkins, S. W., and J. M. Tipping. 1999. Predation by juvenile hatchery salmonids on wild fall Chinook salmon fry in the Lewis River, Washington. Calif. Fish Game 85:124-129.

IPCC (Intergovernmental Panel on Climate Change). 2007. Climate Change 2007, Fourth Assessment Report. Available at: http://www.ipcc.ch/report/ar4/.

Isaak, D. J., C. H. Luce, B. E. Rieman, D. E. Nagel, E. E. Peterson, D. L. Horan, S. Parkes, and G. L. Chandler. 2010. Effects of climate change and wildfire on stream temperatures and salmonid thermal habitat in a mountain river network. Ecological Applications 20:1350-1371.

Iwama G. K. and A. F. Tautz. 1981. A simple growth model for salmonids in hatcheries. Canadian Journal of Fisheries and Aquatic Science 38:649-656.

Jobling, M. 2010. Are compensatory growth and catch-up growth two sides of the same coin? Aquaculture International 18(4):501-510.

Koseki, Y., and I. A. Fleming. 2007. Large-scale frequency dynamics of alternative male phenotypes in natural populations of coho salmon (*Oncorhynchus kisutch*): patterns, processes, and implications. Canadian Journal of Fisheries and Aquatic Sciences 64:743-753.

Liang, X., D. P. Lettenmaier, E. F. Wood, and S. J. Burges. 1994. A simple hydrologically based model of land-surface water and energy fluxes for general-circulation models. Journal of Geophysical Research 99(D7):14,415-14,428.

Luttershmidt, W. I., and V. H. Hutchinson. 1997. The critical thermal maximum: history and critique. Canadian Journal of Zoology 75:1561-1574.

Mantua, N., I. Tohver, and A. Hamlet. 2010. Climate change impacts on streamflow extremes and summertime stream temperature and their possible consequences for freshwater salmon habitat in Washington State. Climatic Change 102:187-223.

Mohseni, O., H. G. Stefan, and T. R. Erickson. 1998. A nonlinear regression model for weekly stream temperatures. Water Resource Research 34:2685-2692.

Namen, S. W., and C. S. Sharpe. 2012 Predation by hatchery yearling salmonids on wild subyearling salmonids in the freshwater environment: A review of studies, two case histories, and implications for management. Environmental Biology of Fishes 94:21-28.

Nash, J. E., and J. V. Sutcliffe. 1970. River flow forecasting through conceptual models. Journal of Hydrology 10:282-290.

Paladino, R. V., J. R. Spotila, J. P. Schubauer and K. T. Kowalski. 1980. The critical thermal maximum: a technique used to elucidate physiological stress and adaptation in fishes. Revue Canadienne de Biologie 39:115-122.

Petersen, J. H., and J. F. Kitchell. 2001. Climate regimes and water temperature changes in the Columbia River: bioenergetic implications for predators of juvenile salmon. Canadian Journal of Fisheries and Aquatic Sciences 58:1831-1841.

Piper, R. G., I. B. McElwain, L. E. Orme, J. P. McCraren, L. G. Fowler, and J. R. Leonard. 1982. Fish hatchery management. US Fish and Wildlife Service, Washington, D.C.

Potter, H., J. Bednarek, M. Cooper, and T. Collier 2017. Entiat National Fish Hatchery Annual Report, 2016. U.S. Fish and Wildlife Service, Entiat WA.

R Core Team. 2013. R: A language and environment for statistical computing. R Foundation for Statistical Computing, Vienna, Austria. URL http://www.R-project.org/.

Rahel, F. J., and J. D. Olden. 2008. Assessing the effects of climate change on aquatic invasive species. Conservation Biology 22(3):521-533.

Scheuerell, M. D., and J. G. Williams. 2005. Forecasting climate-induced changes in the survival of Snake River spring/summer Chinook salmon (*Oncorhynchus tshawytscha*). Fisheries Oceanography 14(6):448-457.

Simpson, W. G., B. M. Kennedy, and K. G. Ostrand. 2009. Seasonal foraging and piscivory by sympatric wild and hatchery-reared steelhead from an integrated hatchery program. Environmental Biology of Fishes 86:473-482.

Vøllestad, L. A., J. Peterson, and T. P. Quinn. 2004. Effects of freshwater and marine growth rates on early maturity in male coho and Chinook salmon. Transactions of the American Fisheries Society 133:495-503.

Weber, E. D., and K. D. Fausch. 2003. Interactions between hatchery and wild salmonids in streams: differences in biology and evidence for competition. Canadian Journal of Fisheries and Aquatic Sciences 60:1018-1036.

Wedemeyer, G. A., editor. 2001. Fish hatchery management, second edition. American Fisheries Society, Bethesda, MD.

Wenger, S. J., D. J. Isaak, J. B. Dunham, K. D. Fausch, C. H. Luce, H. M. Neville, B. E. Rieman, M. K. Young, D. E. Nagel, D. L. Horan, and G. L. Chandler. 2011. Role of climate and invasive species in structuring trout distributions in the interior Columbia River Basin, USA. Canadian Journal of Fisheries and Aquatic Sciences 68(6):988-1008.

Westerling, A. L., H. G. Hidalgo, D. R. Cayan, and T. W. Swetnam. 2006. Warming and earlier spring increases Western U.S. forest wildfire activity. Science 313:940-943. DOI:10.1126/science.1128834

Table B1. Thermal tolerances (°C) of Pacific salmon species (*Oncorhynchus* spp.) reared at Entiat NFH.

Species	Latin Binomial	Life-History Stage	Optimal Temp. Range	Optimal Temp. Growth Range	Spawn Range	Smoltification Threshold
Chinook Salmon	*O. tshawytscha*	adult	6.0 – 14.0 °C		9.0 – 12.3 °C	
		egg/fry	8.4 – 12.4 °C			
		juvenile	8.6 – 15.9 °C	14.0 – 18.4 °C		14.0 °C

Table B2. Thermal ranges (°C) at which common salmon pathogens cause disease in Pacific salmon and Steelhead.

Disease Name	Pathogen Name (causative agent)	Disease Outbreak Temperatures	Minimum Disease Temperatures
Bacteria diseases			
Furunculosis	*Aeromonas salmonicida (A.sal)*	20.0 – 22.0 °C	12.0 °C
Vibriosis	*Vibrio anguillarum*	18.0 – 20.0 °C	14.0 °C
Enteric redmouth disease	*Yersinia ruckeri*	22.0 °C	11.0 – 18.0 °C
Columnaris disease	*Flavobacterium columnaris*	28.0 – 30.0 °C	15.0 °C
Coldwater disease (fin rot)	*Flavobacterium psychrophilum*	4.0 – 10.0 °C	4.0 – 10.0 °C
Bacterial kidney disease	*Renibacterium salmoninarum*		15.0 °C
Fungal diseases			
Saprolegniasis	*Saprolegnia parasitica, Achyla hoferi, Dictyuchus* spp.	15.0 – 30.0 °C	
Parasitic diseases			
Parasitic ichtyobodiasis (Costiasis)	*Ichthyobodo necatrix, I. pyrifornis*	10.0 – 25.0 °C	
White spot disease (Ich)	*Ichthyophthirius multifiliis*	24.0 – 26.0 °C	12.0 – 15.0 °C
Proliferative kidney disease	*Tetracapsuloides bryosalmonae*	16.0 °C	
Ceratomyxosis	*Ceratonova shasta*	15.0 – 25.0 °C	10.0 – 15.0 °C
Viral diseases			
Infectious pancreatic necrosis virus (IPNV) disease	*Aquabirnavirus* sp.	20.0 – 23.0 °C	
Infectious hematopoietic necrosis (IHN) disease	*Novirhadovirus* sp.	13.0 – 18.0 °C	15.0 °C

Table B3. Historical and future mean monthly water temperatures (°C) for the Entiat River adjacent to Entiat NFH. Historical empirical values (°C ± S.D.) are for 2001 – 2006 provided by the hatchery. Predictions for the 2040s represent the mean and range of surface water temperatures derived from statistically downscaled air temperatures from 10 general circulation models (GCMs) under the A1B emissions scenario (IPCC 2007) and regression relationships between air and surface waters (see text for additional details). The historical modeled values are predictions from the air-water regression across the 1915 – 2006 period, and the S.D. shows the variability across that period.

Month	Historical empirical (± S.D.)	Historical modeled (± S.D.)	2040s A1B ensemble (Min. – Max.)
January	1.0 ± 1.2	1.8 ± 1.0	2.5 (2.0 – 2.9)
February	2.2 ± 1.2	2.6 ± 1.1	3.3 (2.7 – 3.9)
March	4.8 ± 1.9	3.9 ± 1.4	4.8 (4.1 – 5.4)
April	7.5 ± 1.6	6.1 ± 1.9	7.6 (6.6 – 9.6)
May	8.0 ± 1.7	9.5 ± 2.3	10.9 (10.4 – 11.9)
June	10.1 ± 2.5	12.7 ± 1.9	14.2 (13.3 – 14.9)
July	15.4 ± 2.7	15.3 ± 1.4	16.7 (16.1 – 17.5)
August	17.3 ± 2.2	15.0 ± 1.4	16.5 (15.8 – 17.2)
September	13.7 ± 2.4	12.6 ± 2.2	14.5 (13.7 – 15.7)
October	8.5 ± 2.5	7.3 ± 2.4	8.8 (8.3 – 9.4)
November	2.8 ± 1.7	3.3 ± 1.3	4.1 (3.9 – 4.4)
December	0.8 ± 1.0	2.0 ± 1.0	2.6 (2.2 – 3.0)

Table B4. Modeled historical and future monthly average air temperatures (T_{ave}, °C), precipitation (PPT, mm), and snow water equivalent (SWE, mm) for the drainage area of the Entiat River upstream from Entiat NFH. Modeled projected future values are ensemble means based on 10 GCMs extracted from daily flux files and weighted by the intersection of the delineated watershed and the 1/16° grid cells underlying the flux files. The historical period is based on the 1915 – 2006 meteorological record, and the 2040s represents a 30-year period (2030 – 2059) centered on the decade of the 2040s. Standard deviation (S.D.) values represent the variability in monthly estimates among the 10 GCMs. Differences (Diff.) are calculated as the 2040s ensemble mean minus the historical mean. An example of the file location for a flux file is: http://warm.atmos.washington.edu/2860/r7climate/hb2860_hybrid_delta_runs/echam5_A1B_2030-2059/fluxes_monthly_summary/fluxsumm_47.78125_-122.90625 .

Month	T_{ave} (°C) Historical	T_{ave} (°C) Projected 2040s (± S.D.)	T_{ave} (°C) Diff.	PPT (mm) Historical	PPT (mm) Projected 2040s (± S.D.)	PPT (mm) Diff.	SWE (mm) Historical	SWE (mm) Projected 2040s (± S.D.)	SWE (mm) Diff.
January	-5.5	-3.7 ± 1.0	1.8	165	178 ± 22	13	222	175 ± 26	-46
February	-3.1	-1.5 ± 1.1	1.6	122	124 ± 17	3	347	271 ± 41	-76
March	-0.2	1.3 ± 0.8	1.5	92	100 ± 6	8	420	319 ± 50	-101
April	3.5	5.2 ± 1.1	1.7	51	56 ± 6	5	433	322 ± 55	-111
May	7.4	9.1 ± 0.7	1.7	38	35 ± 3	-2	350	233 ± 57	-117
June	11.1	13.2 ± 0.7	2.1	29	24 ± 5	-4	189	97 ± 35	-91
July	15.2	18.1 ± 1.2	2.9	16	11 ± 3	-5	54	12 ± 7	-42
August	14.6	17.6 ± 1.0	3.0	19	16 ± 4	-4	5	0 ± 0	-4
September	11.4	14.1 ± 1.0	2.6	33	29 ± 6	-4	1	0 ± 0	-1
October	5.2	7.1 ± 0.4	1.9	85	95 ± 11	10	1	0 ± 0	-1
November	-0.8	0.8 ± 0.3	1.6	158	185 ± 26	28	12	6 ± 1	-6
December	-4.3	-2.5 ± 0.6	1.8	193	206 ± 16	13	86	67 ± 12	-19

Table B5. Projected mean annual flows (cfs) of the Entiat River near Entiat NFH in the 2040s derived from the VIC hydrologic model forced by output from 10 Global Climate Models (GCMs) under the A1B emissions scenario. The historical average is based on the 1915 – 2006 period. Values do not account for other user withdrawals or any hydrologic alterations upstream from the hatchery.

GCM	Mean annual flow in 2040s (cfs)
ccsm3	682
cgcm3	773
cnrm_cm3	720
echam5	697
echo_g	660
hadcm	729
hadgem1	612
ipsl_cm4	782
miroc_3.2	812
pcm1	630
2040s AVERAGE	729
2040s RANGE	612 – 812
Historical AVERAGE	653

Table B6. Mean temperatures of the surface water of the Entiat River at the hatchery intake for Entiat NFH and for groundwater from wells on the facility. Historical values for the Entiat River are empirical data (°C ± S.D.) from 2001 – 2006, and historical values for groundwater wells are empirical data (°C ± S.D.) from 1997 – 2006. Predictions for the 2040s represent the mean and range of surface water temperatures derived from statistically downscaled air temperatures from 10 general circulation models (GCMs) under the A1B emissions scenario (IPCC 2007) and regression relationships between air and surface waters (see text for additional details).

Month	Entiat River historical empirical mean temperature °C ± S.D.	Entiat River historical modeled temperature °C	Entiat River 2040s A1B ensemble mean temperature °C (Min. – Max.)	Groundwater historical empirical mean temperature °C ± S.D.	Groundwater 2040s A1B ensemble mean temperature °C
January	1.0 ± 1.2	1.8	2.5 (2.0 – 2.9)	9.5 ± 0.3	9.7
February	2.2 ± 1.2	2.6	3.3 (2.7 – 3.9)	9.1 ± 0.6	9.1
March	4.8 ± 1.9	3.9	4.8 (4.1 – 5.4)	8.9 ± 1.1	9.0
April	7.5 ± 1.6	6.1	7.6 (6.6 – 9.6)	8.9 ± 0.5	9.0
May	8.0 ± 1.7	9.5	10.9 (10.4 – 11.9)	9.0 ± 0.3	9.1
June	10.1 ± 2.5	12.7	14.2 (13.3 – 14.9)	9.1 ± 0.8	9.2
July	15.4 ± 2.7	15.3	16.7 (16.1 – 17.5)	9.4 ± 0.4	9.5
August	17.3 ± 2.2	15.0	16.5 (15.8 – 17.2)	9.7 ± 0.3	9.9
September	13.8 ± 2.4	12.6	14.5 (13.7 – 15.7)	10.1 ± 0.2	10.3
October	8.5 ± 2.5	7.3	8.8 (8.3 – 9.4)	10.4 ± 0.3	10.5
November	2.8 ± 1.7	3.3	4.1 (3.9 – 4.4)	10.3 ± 0.5	10.5
December	0.8 ± 1.0	2.0	2.6 (2.2 – 3.0	10.1 ± 0.5	10.3

Table B7. Mean monthly water temperatures and water sources experienced by juvenile Chinook Salmon reared at Entiat NFH based on the historical baseline and projected values for the 2040s.

Month	Life-History Stage	Well water percentage	Surface water percentage	Historical baseline water temperatures (°C)	A1B projected 2040s water temperatures (°C)
July	broodstock	100%		9.4	9.5
August	broodstock	100%		9.7	9.9
September	broodstock	100%		10.1	10.3
October	broodstock	100%		10.4	10.5
October	egg/fry	100%		10.4	10.5
November	egg/fry	100%		10.3	10.5
December	egg/fry	100%		10.1	10.3
January	egg/fry	100%		9.5	9.7
February	egg/fry	100%		9.1	9.1
March	egg/fry	100%		8.9	9.0
April	egg/fry	100%		9.0	9.0
May	juvenile	100%		9.0	9.1
June	juvenile	100%		9.1	9.2
July	juvenile	100%		9.4	9.5
August	juvenile	100%		9.7	9.9
September	juvenile	100%		10.1	10.3
October	juvenile	100%		10.4	10.5
November	juvenile	15%	85%	3.9	5.1
December	juvenile	15%	85%	2.2	3.8
January	juvenile	20%	80%	2.7	3.9
February	juvenile	20%	80%	3.5	4.5
March	juvenile	20%	80%	5.6	5.8
April	smolt	20%	80%	7.8	7.8

Table B8. Monthly percent size differences of juvenile Chinook Salmon reared at Entiat NFH in the 2040s under a future temperature scenario relative to baseline historical water temperatures.

Month	Life-History Stage	Weight (g)	Length (mm)
July	Juvenile	2.0%	0.6%
August	Juvenile	3.0%	1.0%
September	Juvenile	3.4%	1.1%
October	Juvenile	3.2%	1.1%
November	Juvenile	7.1%	2.3%
December	Juvenile	12.7%	4.0%
January	Juvenile	16.4%	5.1%
February	Juvenile	18.5%	5.8%
March	Juvenile	17.1%	5.4%
April	Smolt	15.6%	4.9%

Table B9, Part A. Mean empirical historical and modeled historical flow and density index values and constituent variables for Summer Chinook Salmon at Entiat NFH. Rearing (Rear.) parameters are listed in columns 3 – 5. Empirical historical values (Emp.) are listed in columns 6 – 10. Modeled historical values (Mod.) are listed in columns 11 – 14.

Time step (*i*)	Month[a]	Rear. N_i [b]	Rear. C_i(ft^3)[c]	Rear. d_i [d]	Emp. L_i [e]	Emp. W_i [f]	Emp. GPM_i[g]	Emp. DI_i [h]	Emp. FI_i [i]	Mod. L_i [j]	Mod. W_i [k]	Mod. DI_i [l]	Mod. FI_i[m]	r_i[n]
1	Jun	446,554	8,880	30	2.53	2.41	2,025	0.11	0.46	2.36	2.43	0.11	0.50	0.92
2	Jul	446,242	8,880	31	2.98	3.90	1,804	0.14	0.71	2.84	4.29	0.17	0.82	0.87
3	Aug	445,885	26,640	31	3.66	8.57	1,592	0.09	0.48	3.35	7.02	0.08	0.43	1.12
4	Sep	445,573	26,640	30	4.22	14.01	1,579	0.12	0.69	3.85	10.71	0.10	0.58	1.19
5	Oct	445,377	26,640	31	4.58	17.94	1,579	0.14	0.81	4.38	15.83	0.13	0.75	1.08
6	Nov	445,163	44,400	30	4.59	18.87	3,530	0.09	0.38	4.54	17.69	0.09	0.36	1.05
7	Dec	444,700	44,400	31	4.55	18.59	3,434	0.09	0.39	4.61	18.60	0.09	0.38	1.01
8	Jan	444,211	44,400	31	4.53	18.35	3,866	0.09	0.34	4.72	19.91	0.09	0.36	0.96
9	Feb	443,776	44,400	28	4.65	19.61	4,110	0.09	0.33	4.85	21.60	0.10	0.35	0.95
10	Mar	443,563	44,400	31	5.11	25.92	4,374	0.11	0.38	5.10	25.21	0.11	0.37	1.03
11	Apr	443,474	44,400	30	5.26	28.46	4,414	0.12	0.40	5.45	30.79	0.12	0.42	0.96

[a] Calendar month in rearing cycle.

[b] Numbers of post-hatch juvenile fish or abundance (N_i) based on hatchery averages during 2013 – 2017 brood years.

[c] Mean hatchery capacity (C_i) used during 2013 – 2017 brood years based on the number of raceways, their sizes, and water depth. The number of individual raceways in use in any month can be calculated as $C_i \div 1{,}480$ ft^3.

[d] Number of days (d_i) in the monthly time-step *i*.

[e] Empirical mean fish length (L_i) in inches, at the end of each monthly time-step *i* averaged over the 2013 – 2017 brood years. Empirical data indicated very little growth during Nov – Feb, and in some years the mean length of measured fish decreased across these months which resulted in average table values here that suggest fish lost length in Dec and Jan.

[f] Empirical mean fish weight (W_i) in grams, at the end of each monthly time-step *i* averaged over the 2013 – 2017 brood years.

[g] Empirical mean total flow rates through the hatchery (GPM_i) in gallons per minute at each monthly time-step *i* averaged over the 2013 – 2017 brood years for months Jun – Oct, and averaged over 2013 – 2017. For Entiat NFH, the actual flow per raceway usually depends on the number of A-bank raceways receiving water. For these calculations, the number of A-bank raceways in use was 6 during Jun-Oct and 10 during Nov-Apr; thus, the average flow per raceway was 337.5 GPM during Jun (=2,025 GPM total ÷ 6 raceways) and was 353 GPM during Nov (= 3,530 GPM total ÷ 10 raceways). There was serial re-use such that there were 18 total raceways in use during Aug-Oct and 30 total raceways in use during Nov-Apr.

[h] Empirical density index (DI_i) at time-step *i* based on C_i, N_i, and fish size averaged across the 2013 – 2017 brood years.

[i] Empirical mean flow index (FI_i) at time-step i based on flow per raceway, N_i and fish size averaged over the 2013 – 2017 brood years.

[j] Modeled historical or projected future mean fish length (L_i) in inches, at the end of each monthly time-step i.

[k] Modeled historical or projected future mean fish weight (W_i) in grams, at the end of each monthly time-step i.

[l] Modeled historical density index (DI_i) at time-step i.

[m] Modeled historical flow index (FI_i) at time-step i.

[n] Bias correction factors are the ratio between empirical mean index values and simulated historical values, (see footnote at bottom of page 14.

$$r_i = rFI_i = \frac{FI_i \text{ mean empirical historical}}{FI_i \text{ modeled historical}} = rDI_i = \frac{DI_i \text{ mean empirical historical}}{DI_i \text{ modeled historical}}$$

For additional details, see Online Resource 2 at Hanson and Peterson (2014).

Table B9, Part B. Bias-corrected future (2040s) modeled mean length, mean weight, and flow and density index values for Summer Chinook Salmon at Entiat NFH under four water availability scenarios (see text for details). Modeled values under Scenario A are listed in columns 3 – 6. Fish size and DI_i for Scenarios B, C, and D are the same as for Scenario A. Bias-corrected flow and density index values are shown graphically in Figure 18.

Time step (*i*)	Month[a]	L_i [b]	W_i [c]	DI_i [d]	FI_i [e]	Scenario B FI_i [e]	Scenario C FI_i [e]	Scenario D FI_i [e]
1	Jun	2.36	2.43	0.11	0.46	0.46	0.46	0.58
2	Jul	2.86	4.37	0.15	0.72	0.72	0.72	1.68
3	Aug	3.38	7.24	0.09	0.49	0.49	0.49	0.97
4	Sep	3.89	11.08	0.13	0.70	0.70	0.70	1.02
5	Oct	4.42	16.34	0.15	0.83	0.83	0.83	0.85
6	Nov	4.64	18.95	0.10	0.40	0.27	0.27	0.42
7	Dec	4.80	20.96	0.10	0.42	0.25	0.25	0.46
8	Jan	4.96	23.17	0.10	038	0.20	0.20	0.42
9	Feb	5.13	25.59	0.10	0.37	0.21	0.21	0.42
10	Mar	5.37	29.53	0.12	0.42	0.28	0.28	0.47
11	Apr	5.72	35.59	0.13	0.44	0.33	0.33	0.48

[a] Calendar month in rearing cycle.

[b] Modeled historical or projected future mean fish length (L_i) in inches, at the end of each monthly time-step *i*.

[c] Modeled historical or projected future mean fish weight (W_i) in grams, at the end of each monthly time-step *i*.

[d] Modeled future density index (DI_i) at time-step *i* adjusted using r_i.

[e] Modeled future flow index (FI_i) at time-step *i* adjusted using r_i.

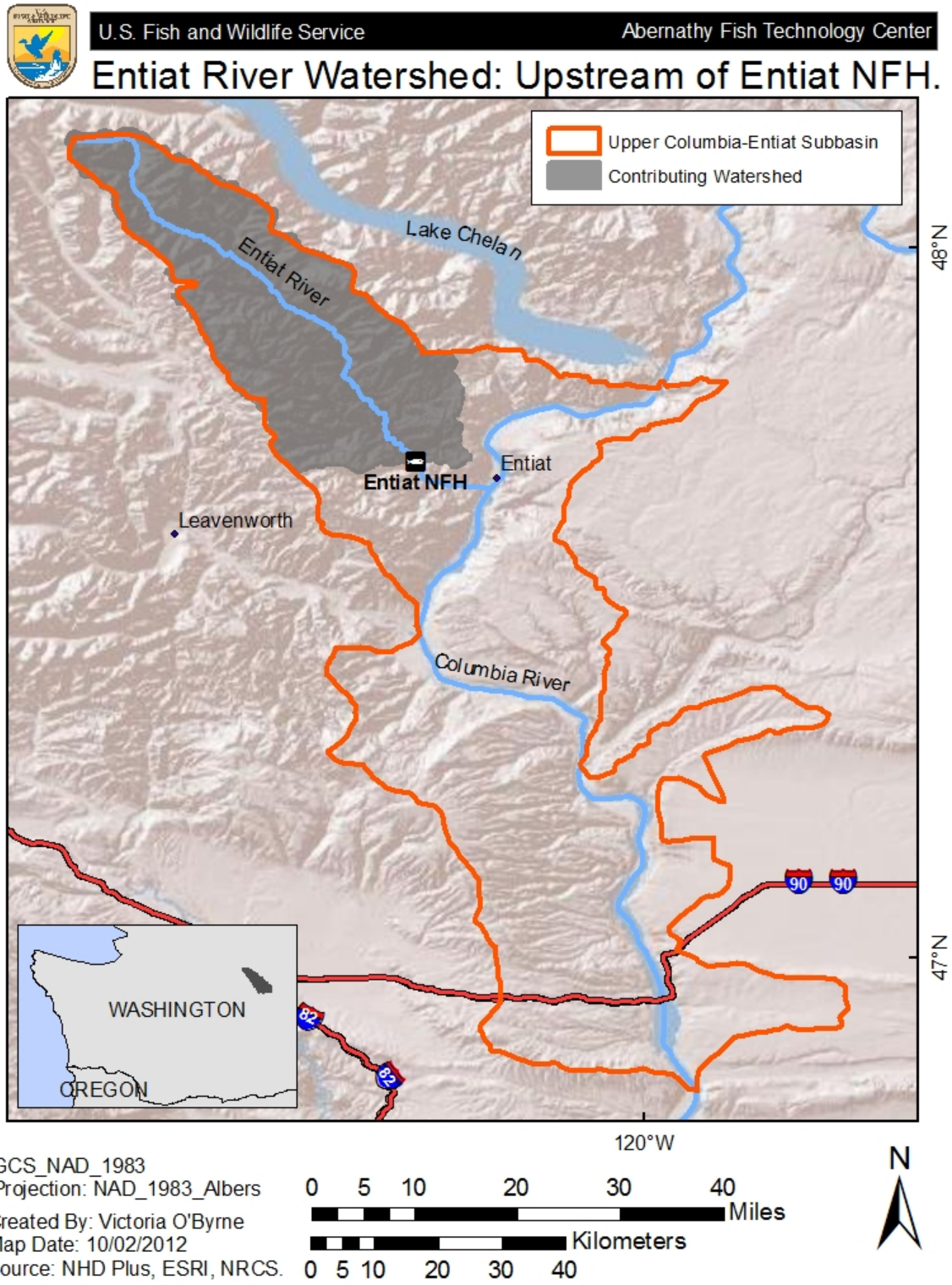

Figure B1. The Entiat River contributing watershed (gray shaded area) and Entiat NFH in northeastern Washington.

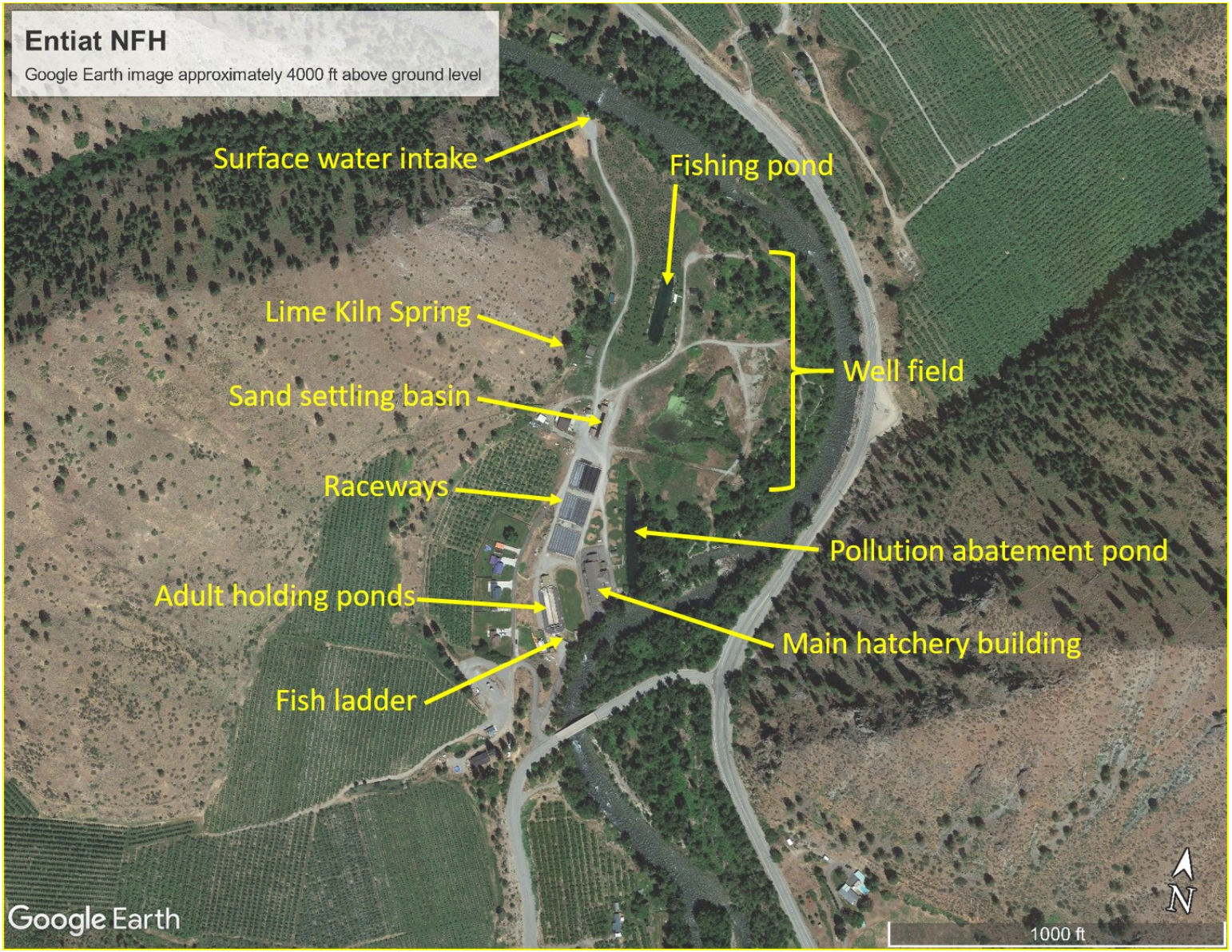

Figure B2. Aerial view of Entiat NFH and the Entiat River, which is flowing from top to bottom.

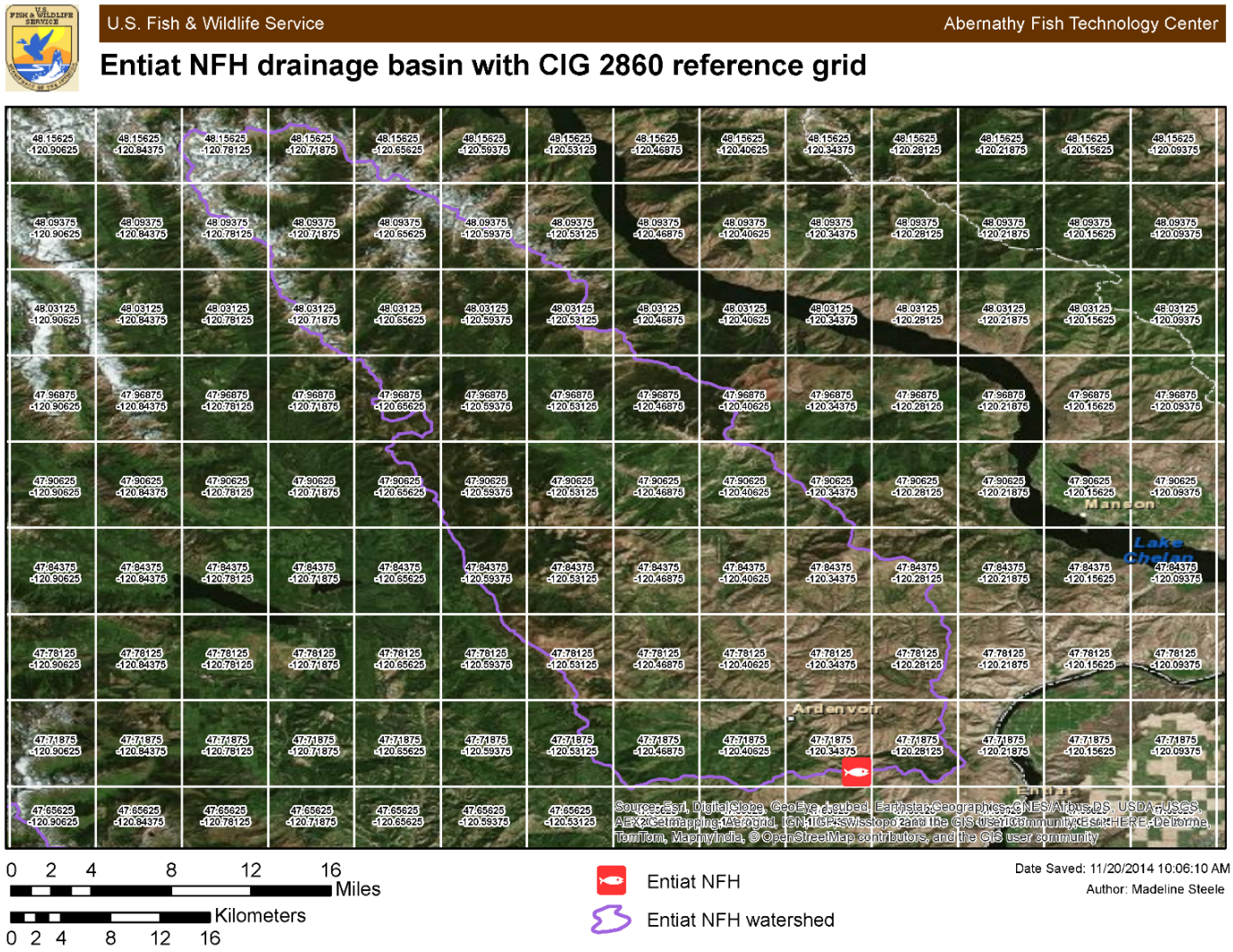

Figure B3. The Entiat River watershed showing the intersection between the watershed delineation and the 1/16° grid cells to which the climate data were downscaled.

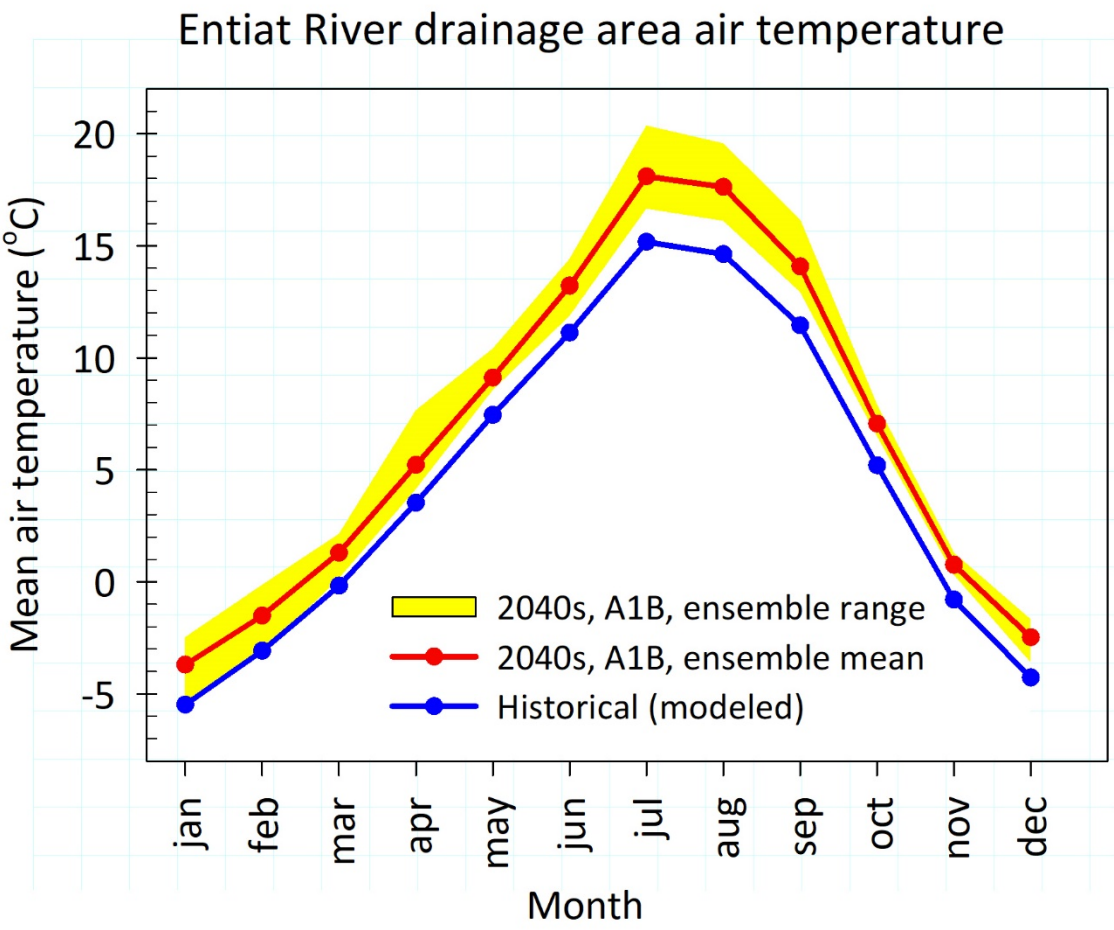

Figure B4. Modeled mean monthly air temperatures (°C) across the Entiat River watershed upstream from Entiat NFH based on an ensemble of 10 GCMs. Values are weighted by the intersection of the delineated watershed and the 1/16° grid cells underlying the flux files. The historical period is based on the 1915 – 2006 meteorological record, and the 2040s represents a 30-year period (2030 – 2059) centered on the decade of the 2040s.

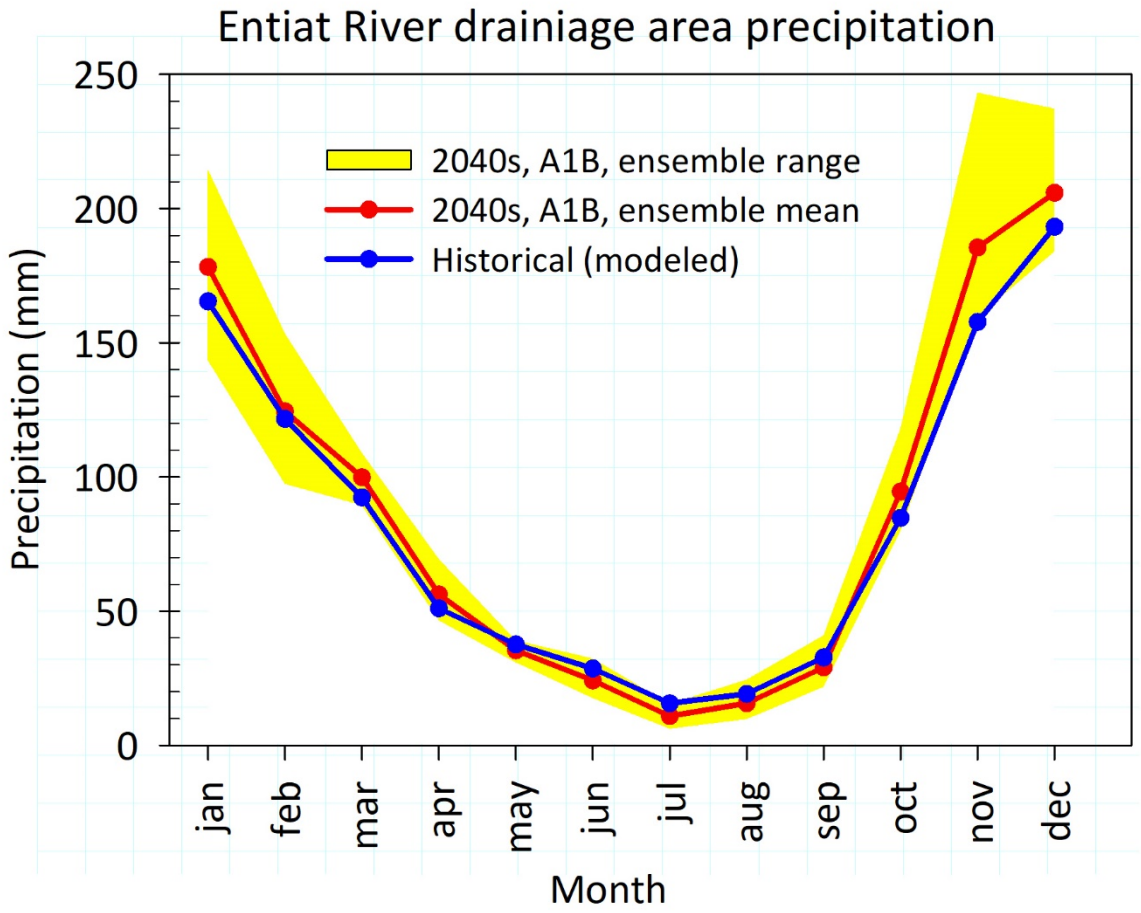

Figure B5. Modeled mean monthly precipitation (mm) across the Entiat River watershed upstream from Entiat NFH based on an ensemble of 10 GCMs. Values are weighted by the intersection of the delineated watershed and the 1/16° grid cells underlying the flux files. The historical period is based on the 1915 – 2006 meteorological record, and the 2040s represents a 30-year period (2030 – 2059) centered on the decade of the 2040s.

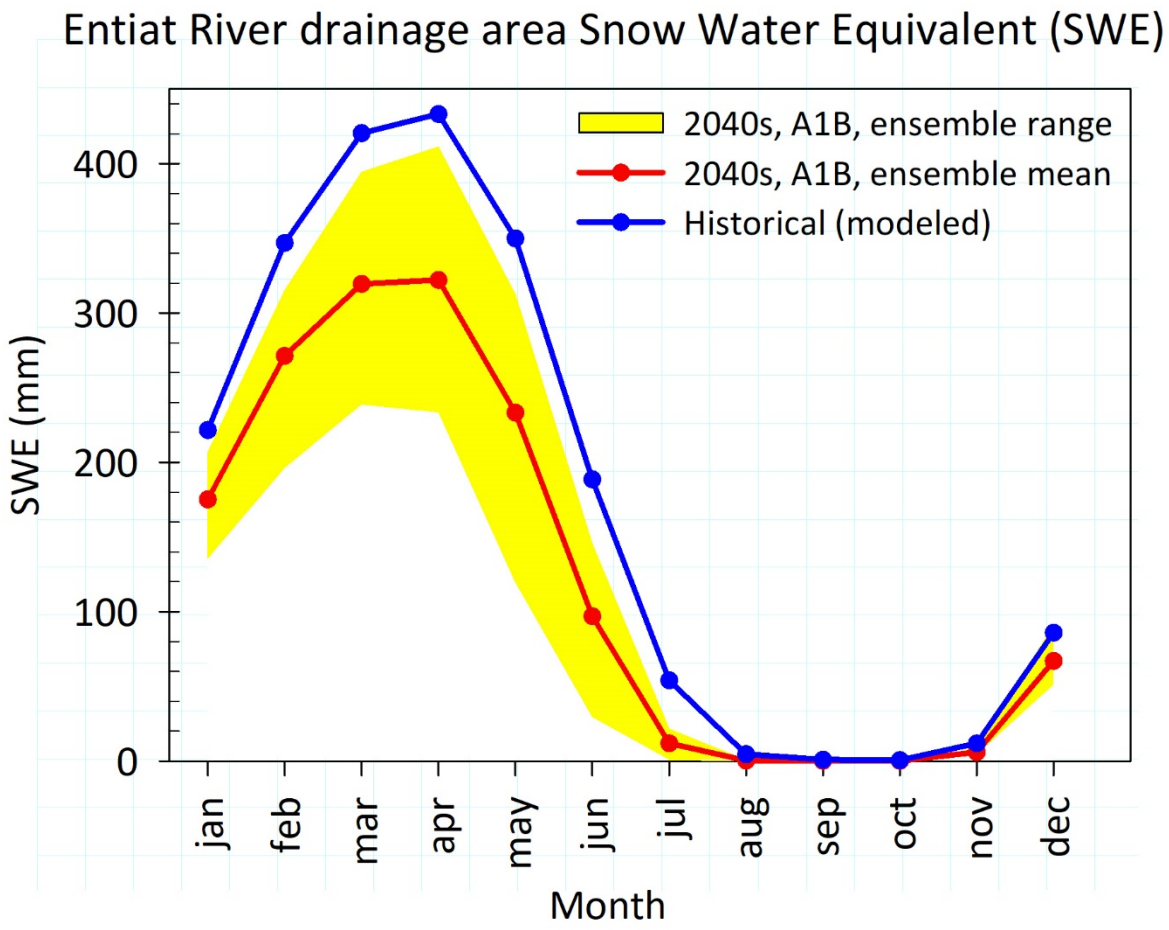

Figure B6. Modeled mean monthly snow water equivalent (SWE) (mm) across the Entiat River watershed upstream from Entiat NFH based on an ensemble of 10 GCMs. Values are weighted by the intersection of the delineated watershed and the 1/16° grid cells underlying the flux files. The historical period is based on the 1915 – 2006 meteorological record, and the 2040s represents a 30-year period (2030 – 2059) centered on the decade of the 2040s.

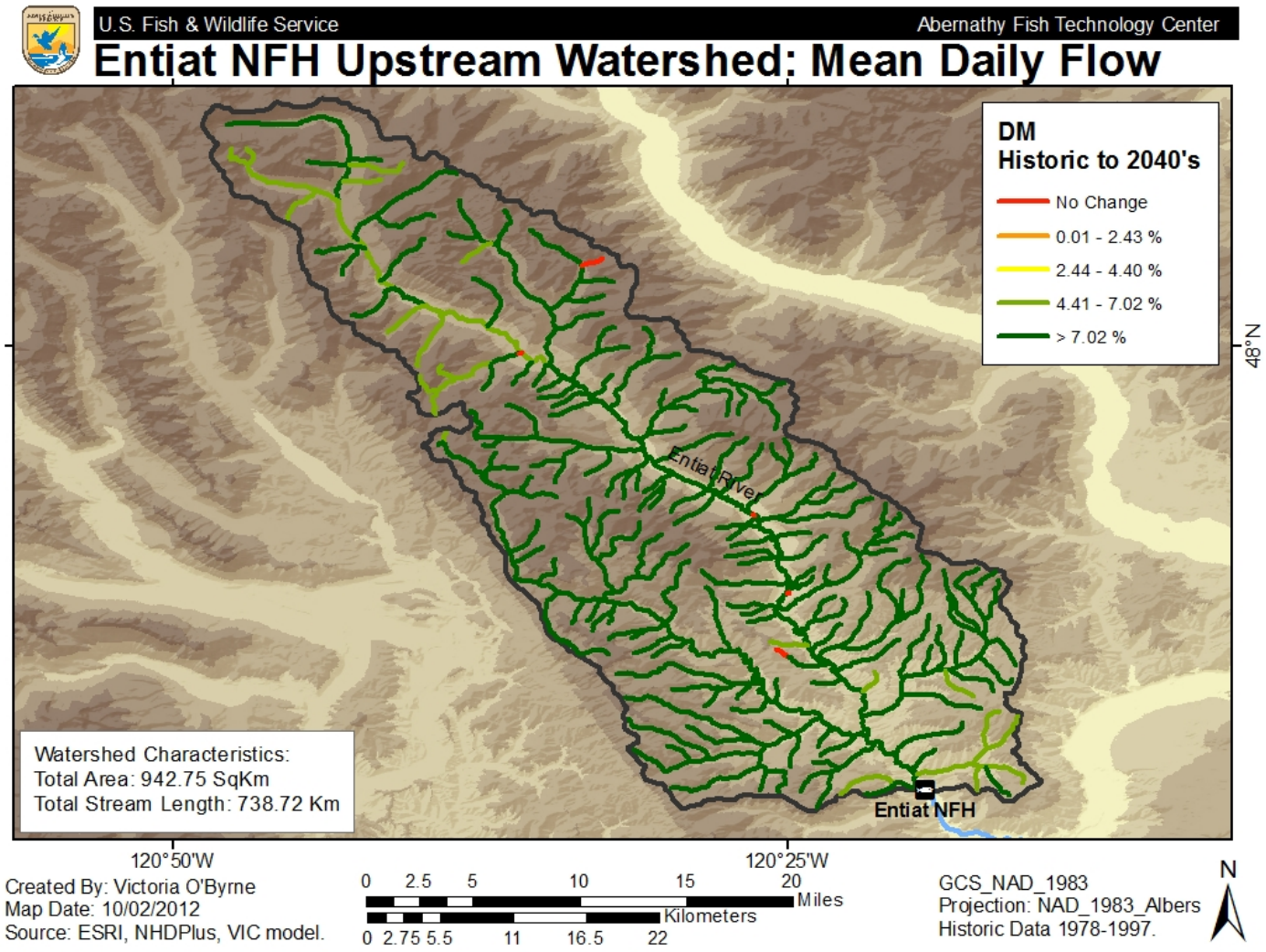

Figure B7. Projected change in mean daily flow (DM, in %) for the Entiat River basin upstream from Entiat NFH between the 1980s and 2040s time periods. Data are from VIC hydrologic model (Wenger et al. 2011) and the historical reference period is 1978 – 1997.

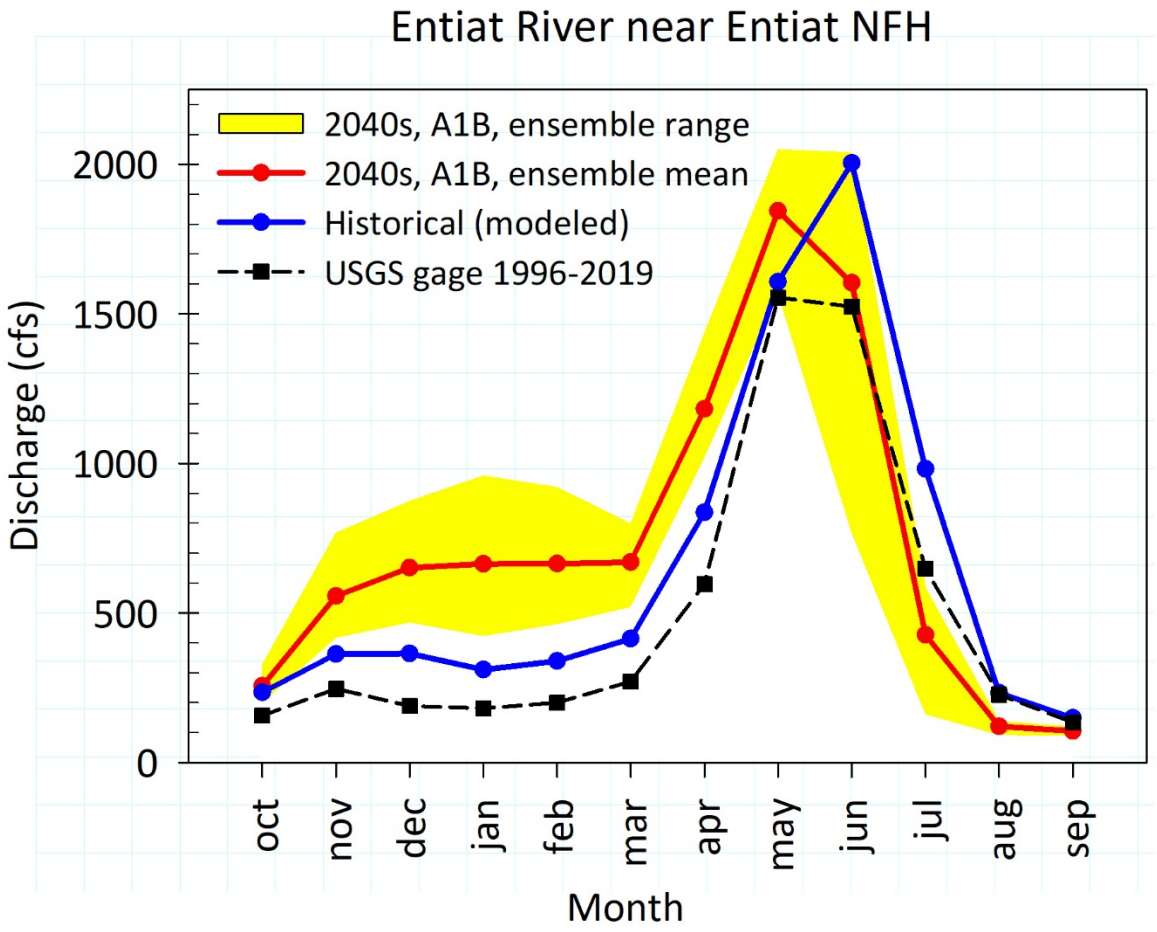

Figure B8. Modeled mean monthly surface flow (cfs) in the Entiat River adjacent to Entiat NFH based on raw Variable Infiltration Capacity (VIC) simulations. Projected (2040s) surface flows are based on the VIC model forced by output from an ensemble of 10 general circulation models (GCMs) under the A1B greenhouse gas emissions scenario. Modeled flow data are routed to the location of the hatchery. The modeled historical period is based on the 1915 – 2006 meteorological record, and the 2040s represents a 30-year period (2030 – 2059) centered on the decade of the 2040s. Empirical flows for the Entiat River are from the period of record (1996 – 2019) for USGS gage # 12452990 downstream from the hatchery. Modeled flows do not account for other water withdrawals in the basin (e.g., irrigation, industry, municipal uses).

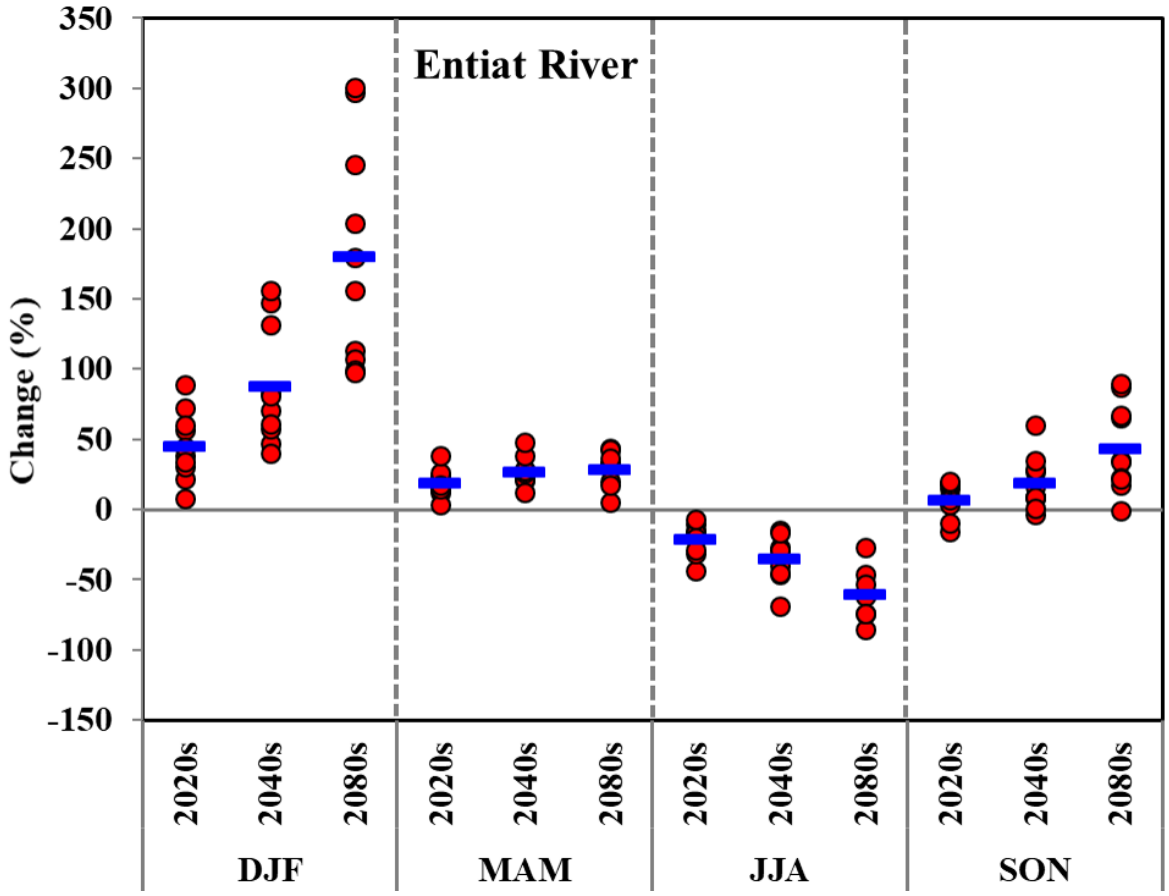

Figure B9. Projected percent change in mean seasonal flow in the Entiat River adjacent to the Entiat NFH based on raw Variable Infiltration Capacity (VIC) simulations for the 30-year periods centered on the 2020s, 2040s, and 2080s. Flow projections are based on the VIC model forced by output from an ensemble of 10 general circulation models (GCMs) under the A1B greenhouse gas emissions scenario. Seasons depicted are winter (December, January, February – DJF), spring (MAM), summer (JJA), and fall (SON), where the letters denote the first initial of each month in the season. Red dots (●) are the projections for the individual GCMs with hybrid-delta downscaling, and the blue horizontal dash (—) is the ensemble average. Differences (percentage change) are relative to the 1915 – 2006 historical period.

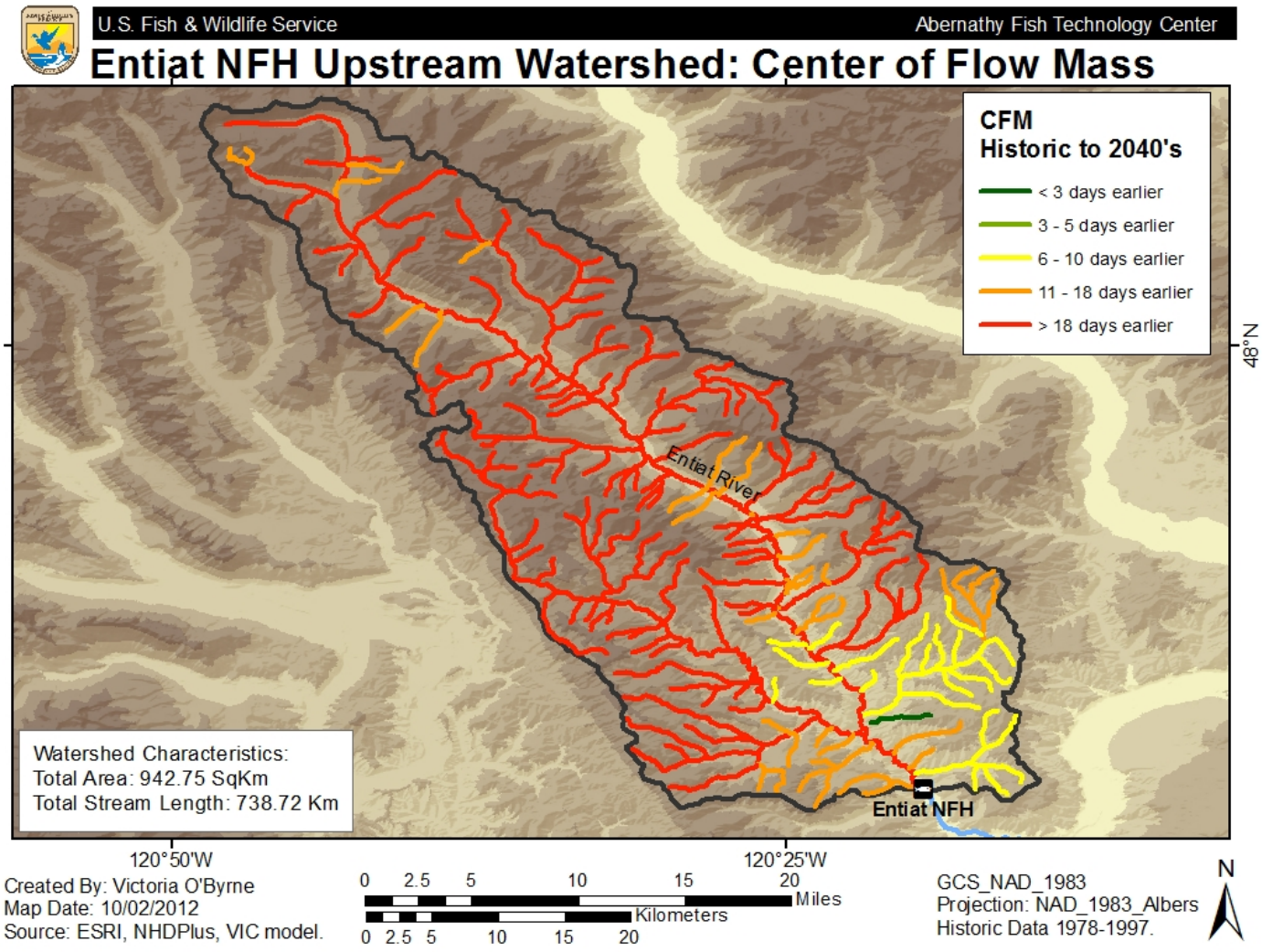

Figure B10. Projected change in the timing of snowmelt runoff (date of center of flow mass, CFM) for the Entiat River basin upstream from Entiat NFH between the 1980s and 2040s time periods. Data are from VIC hydrologic model (Wenger et al. 2011) and the historical reference period is 1978 – 1997.

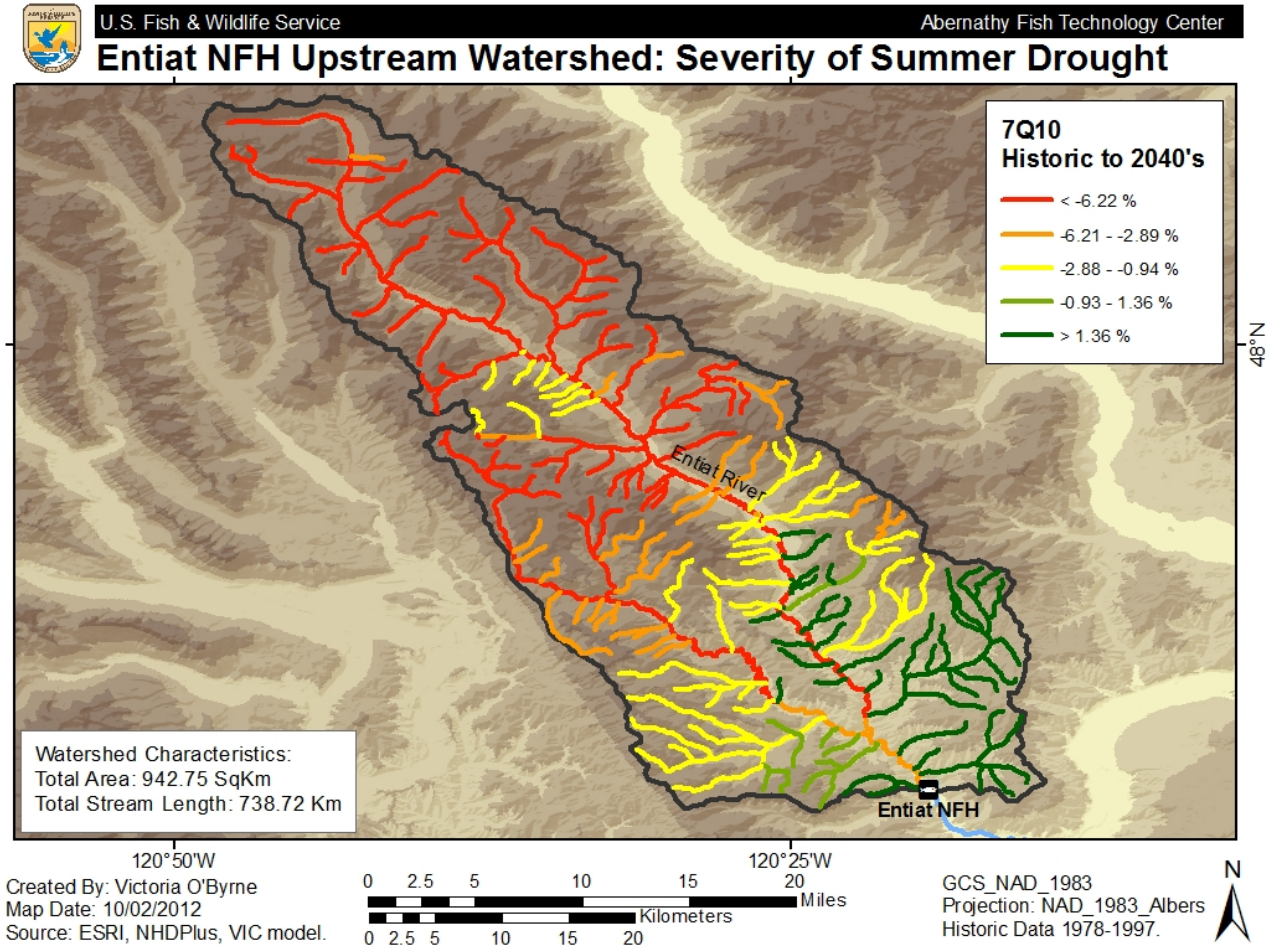

Figure B11. Projected change in the severity of summer drought (7-day low flow 10-yr return interval [7Q10]) for the Entiat River basin upstream from Entiat NFH between the 1980s and 2040s periods. A negative value indicates a lower flow (more severe drought). Data are from VIC hydrologic model (Wenger et al. 2011) and the historical reference period is 1978 – 1997

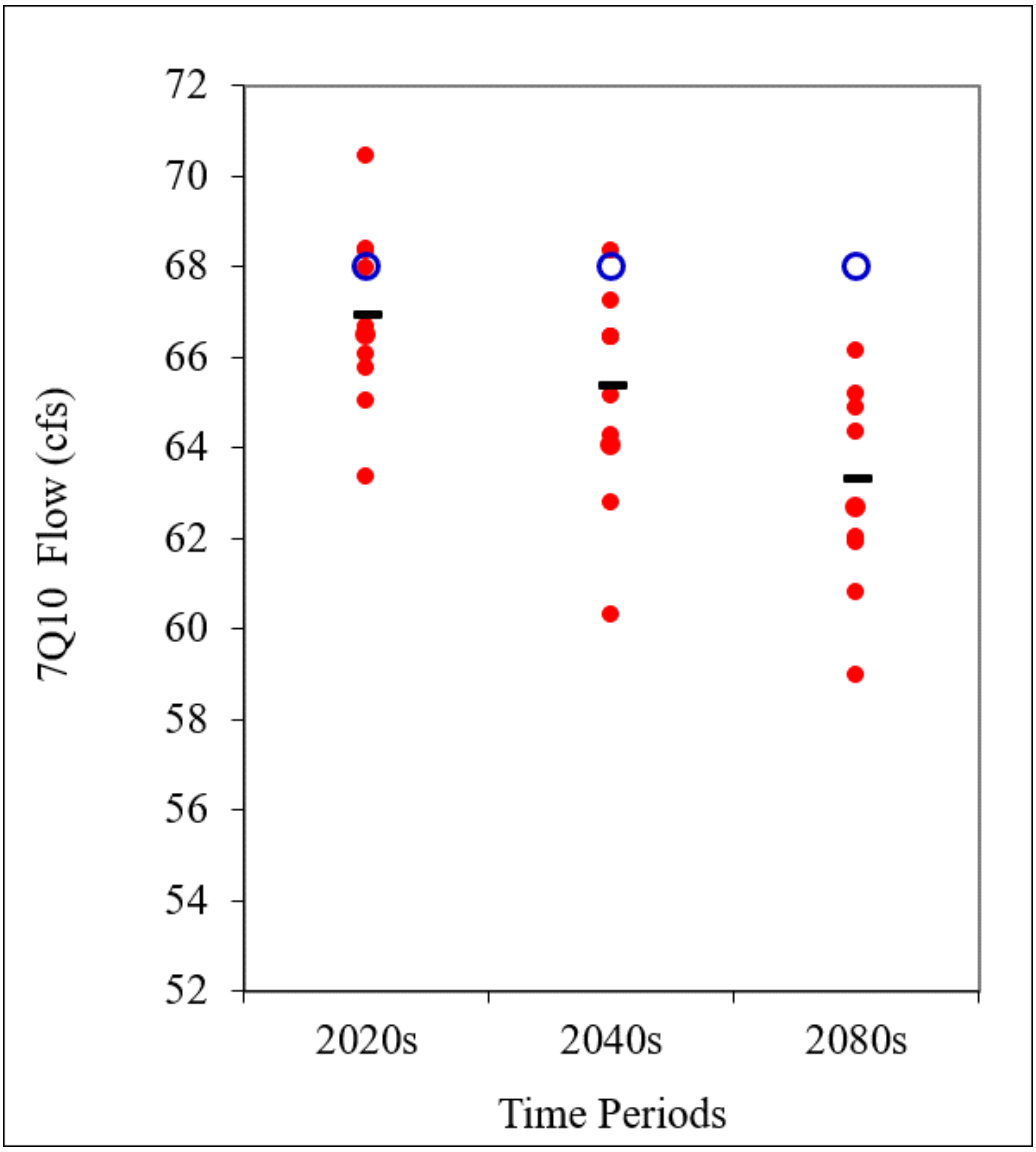

Figure B12. Projected flow rate (cfs) for the 7-day low flow with a 10-yr return interval (7Q10) in Entiat River adjacent to the Entiat NFH based on raw Variable Infiltration Capacity (VIC) simulations for the 2020s, 2040s, and 2080s. Flow projections are based on the VIC model forced by output from an ensemble of 10 general circulation models (GCMs) under the A1B greenhouse gas emissions scenario. Red dots (●) are the projections for the individual GCMs with hybrid-delta downscaling, the black horizontal dash (—) is the ensemble average, and the open blue circle (○) is the historical mean value.

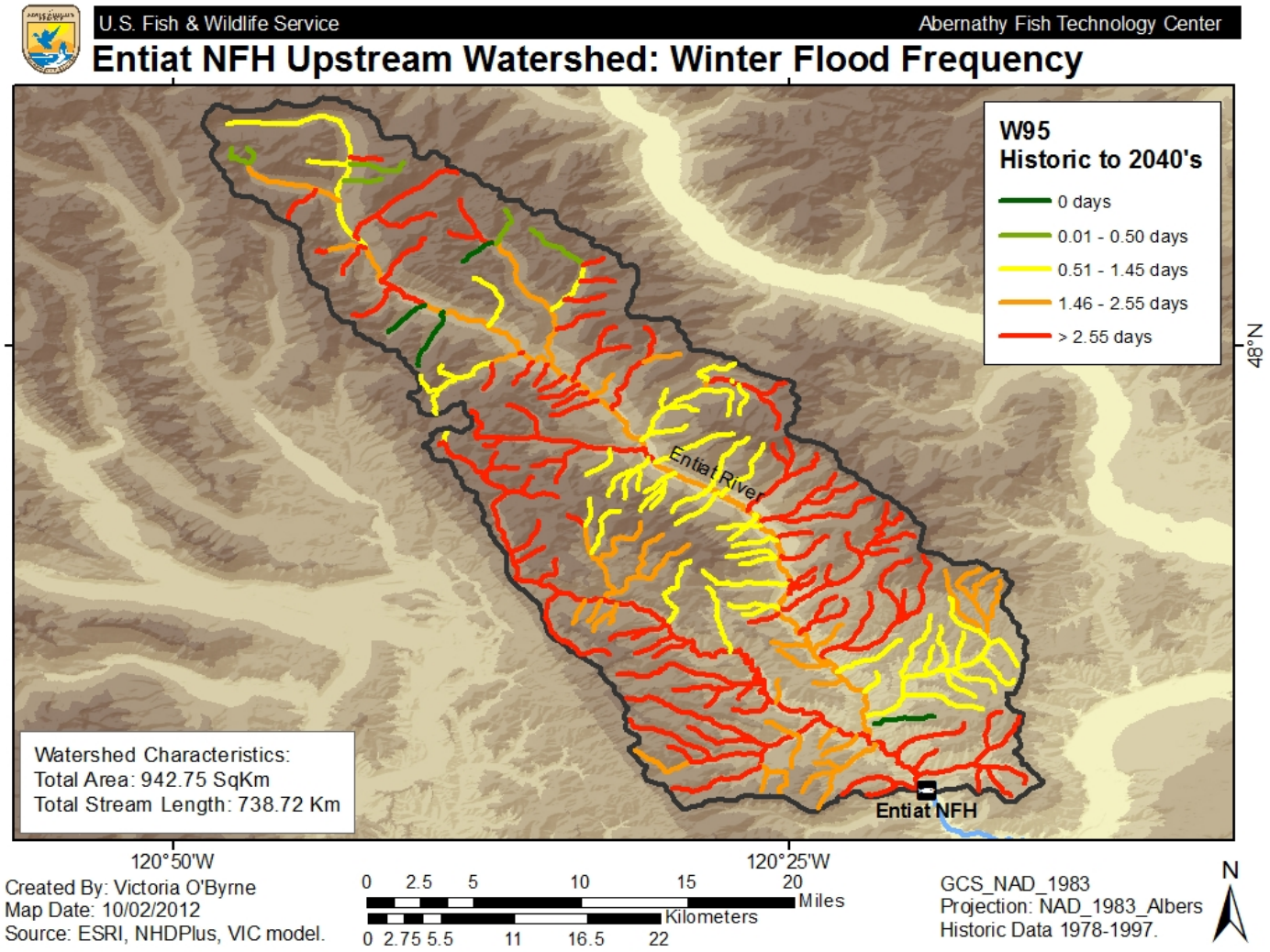

Figure B13. Projected change in the frequency of winter high flows (W95; i.e., number of days in winter that modeled flow was in the top 5% of annual flows) for the Entiat River basin upstream from Entiat NFH between the 1980s and 2040s periods. Data are from VIC hydrologic model (Wenger et al. 2011) and the historical reference period is 1978 – 1997.

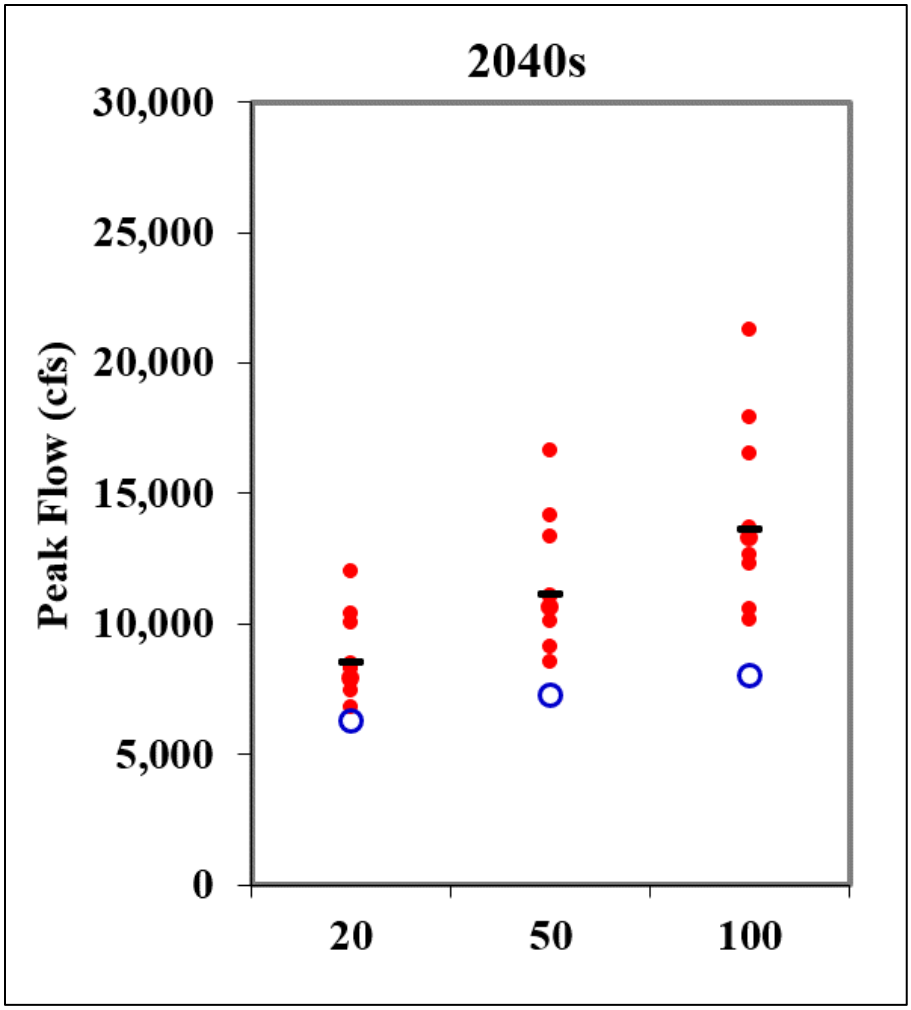

Figure B14. Magnitude (cfs) of 20, 50, and 100-year recurrence interval floods for Entiat River adjacent to the Entiat National Fish Hatchery based on raw Variable Infiltration Capacity (VIC) simulations for the 2040s. Flow projections are based on the VIC model forced by output from an ensemble of 10 general circulation models (GCMs) under the A1B greenhouse gas emissions scenario. Red dots (●) are the projections for the individual GCMs with hybrid-delta downscaling, the black horizontal dash (—) is the ensemble average, and the open blue circle (○) is the historical mean.

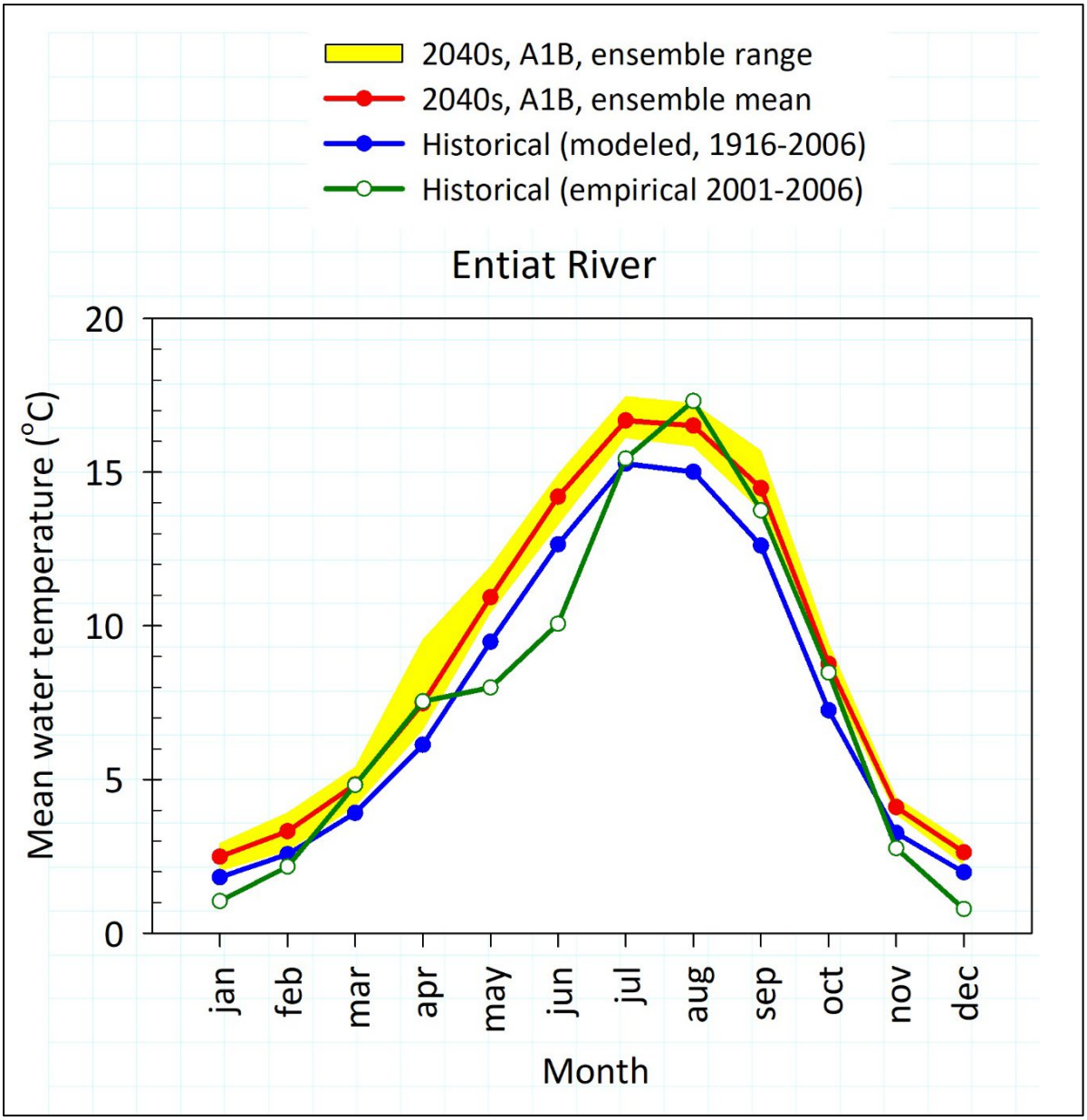

Figure B15. Measured and modeled water temperatures (°C) in the Entiat River adjacent to Entiat NFH. Modeled estimates of projected (2040s) water temperatures were generated via the regression model and are forced by output from an ensemble of 10 GCMs under the A1B greenhouse gas emissions scenario. The modeled historical period is based on the 1915 – 2006 meteorological record, and the 2040s represents a 30-year period (2030 – 2059) centered on the decade of the 2040s. Empirical point estimates based on thermograph data during 2001 – 2006 (green plot) are shown for reference. The simulated historical values are presented to show the variability across 1915 – 2006.

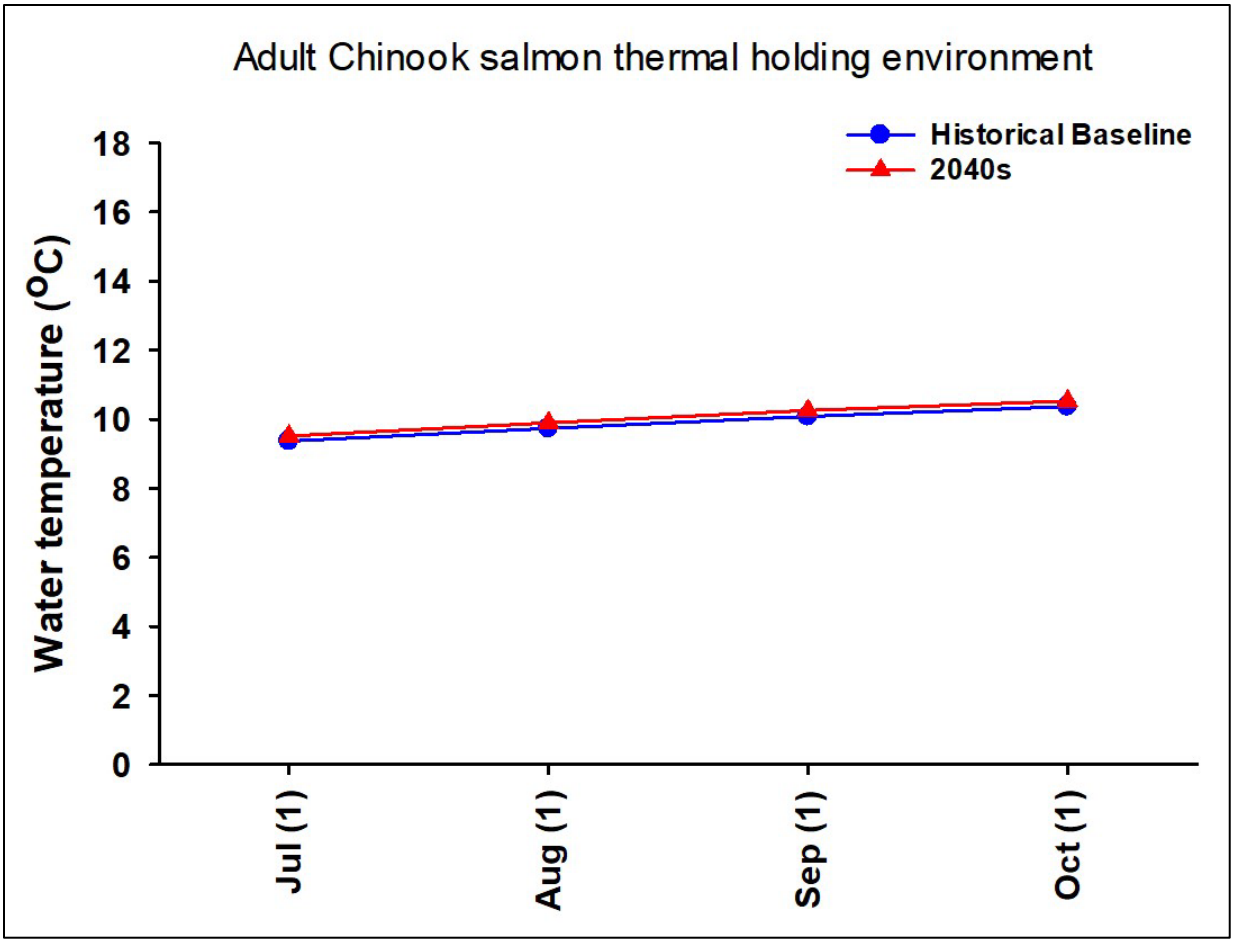

Figure B16. Comparison of the mean water temperatures (°C) experienced by adult Summer Chinook Salmon broodstock held at Entiat NFH based on the simulated historical baseline and projected values for the 2040s under the A1B emission scenario.

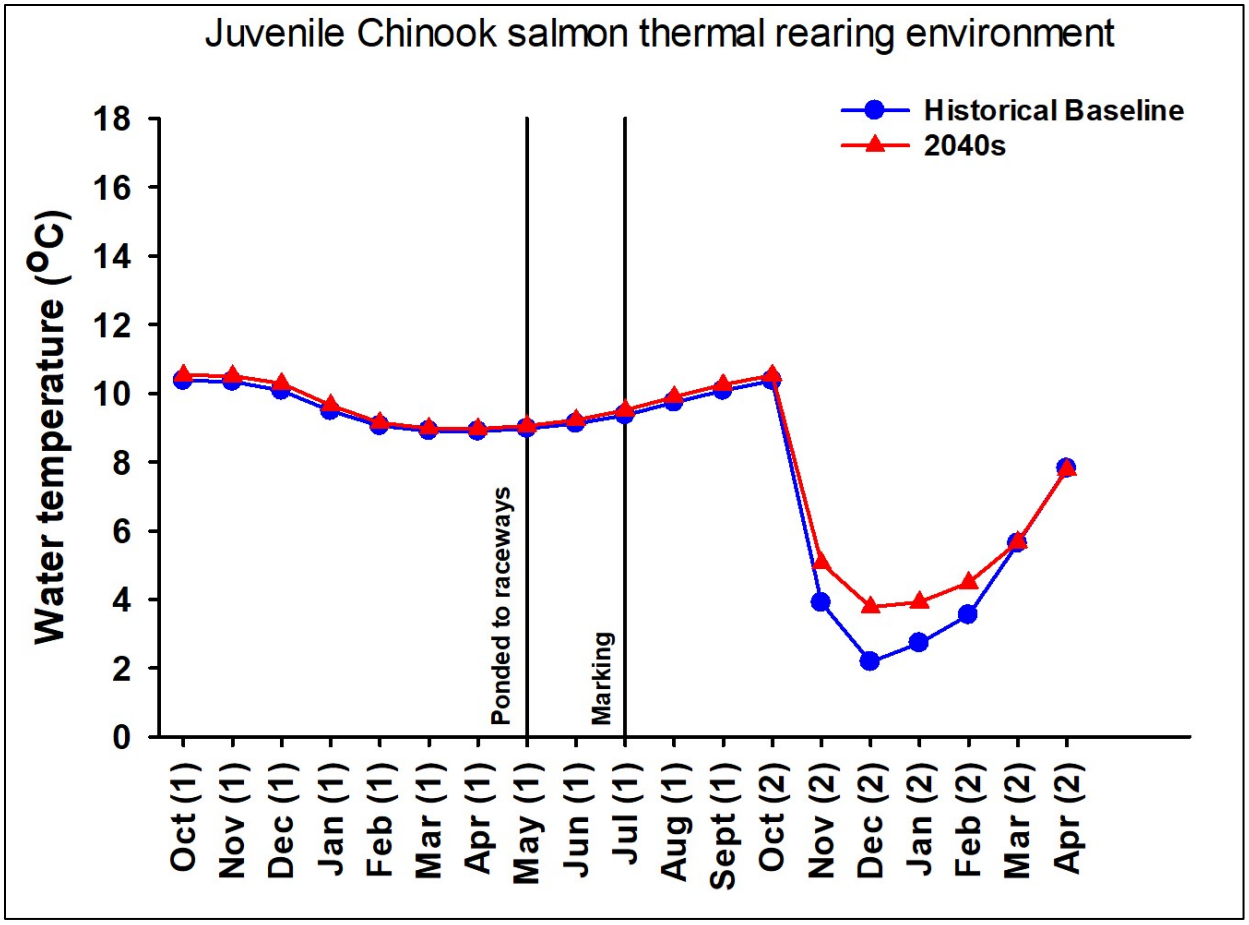

Figure B17. Comparison of the mean water temperatures (°C) experienced by juvenile Summer Chinook Salmon reared at Entiat NFH based on the simulated historical baseline and projected values for the 2040s under the A1B emission scenario and for a future temperature scenario.

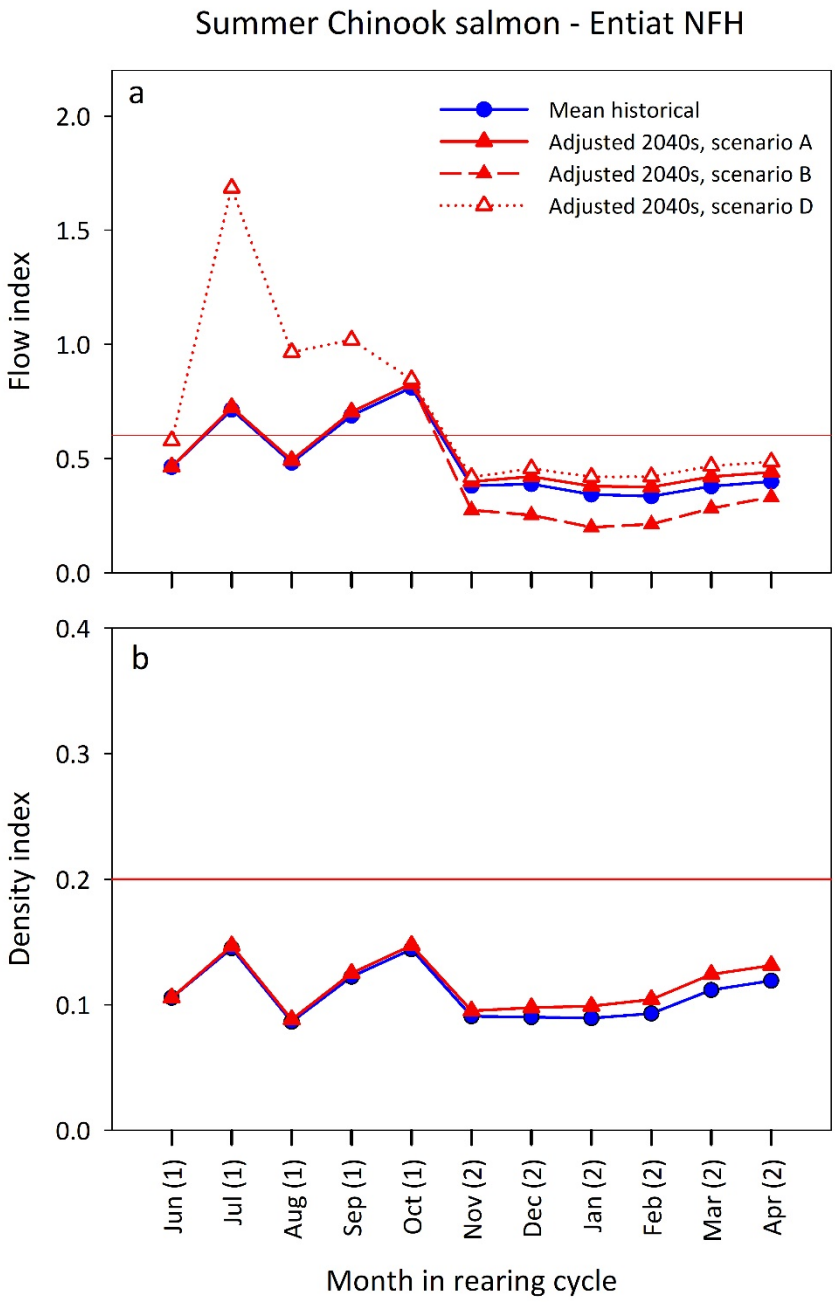

Figure B18. Mean historical and bias-corrected future flow index (a) and density index (b) values for Summer Chinook Salmon at Entiat NFH based on average rearing conditions during 2013 – 2017 brood years and three future water availability scenarios. Values for the 2040s have been bias corrected by multiplying the uncorrected future values by the ratio: (observed mean historical value 2013 – 2017 brood years) / (modeled historical value). See Table B9 for bias correction values. For flow index (panel a), Scenarios B and C produced identical results as indicated by the dashed Scenario B line. The horizontal line in each plot represents the upper-limit, fish health guideline for Summer Chinook Salmon.

This page is intentionally blank.